Hindawi
Journal of Chemistry
Volume 2021, Article ID 6051116, 23 pages
https://doi.org/10.1155/2021/6051116

Research Article

Isothermal and Kinetic Investigation of Exploring the Potential of Citric Acid-Treated *Trapa natans* and *Citrullus lanatus* Peels for Biosorptive Removal of Brilliant Green Dye from Water

Muhammad Sadiq Hussain, Rabia Rehman, and Muhammad Imran

Centre for Inorganic Chemistry, School of Chemistry, University of the Punjab, Quaid-e-Azam Campus, Lahore 54590, Pakistan

Correspondence should be addressed to Rabia Rehman; grinorganic@yahoo.com

Received 27 April 2021; Revised 16 September 2021; Accepted 5 October 2021; Published 1 November 2021

Academic Editor: Alberto Figoli

Trapa natans peels (TNPs) and *Citrullus lanatus* peels (CLPs) were utilized for the biosorptive removal of brilliant green dye (BGD), after modifying with citric acid. Characterization and surface morphology were studied by Fourier transform infrared spectroscopy and scanning electron microscopy. For the removal of BGD by citric acid-treated *Trapa natans* peels (CA-TNPs), the optimum conditions were obtained with adsorbent dose 0.8 g, contact time 25 minutes, initial pH 5, temperature 30°C, and agitation speed 100 rpm, while for the citric acid-treated *Citrullus lanatus* peels (CA-CLPs), adsorbent dose 0.8 g, contact time 20 minutes, pH 5, temperature 30°C, and agitation speed 100 rpm gave optimum results. The q_{max} values obtained were 108.6, 128, 144.9, and 188.68 mg/g for R-TNP, CA-TNP, R-CLP, and CA-CLP, respectively, while the correlation coefficient (R^2) values obtained were 0.985, 0.986, 0.985, and 0.998 for R-TNP, CA-TNP, R-CLP, and CA-CLP, respectively. These favor the Langmuir isotherm and pseudo-second-order kinetics, with negative (ΔG^0) values of all adsorbents, determining that the adsorption phenomenon is exothermic and spontaneous in nature. Both citric acid-treated peels of *Trapa natans* and *Citrullus lanatus* were found suitable for bulk-scale eradication of hazardous, toxic, and carcinogenic basic cationic dyes.

1. Introduction

There are many natural resources in our environment, but water is a very essential constituent and has a number of conflicting demands. Highly skilled management is needed to secure our water resources and to save aquatic life and mankind. The spread of waterborne diseases through water pollution is the major cause of the worldwide death of living organisms [1]. It is reported in the literature that low-cost and efficient adsorbents such as *Eugenia jambolana* seeds and *Citrullus lanatus* peels were used for the detoxification of basic blue 9 dye from aqueous media [2]. During the dyeing and processing of fabrics, colored water is discharged into the water resources through wastewaters. It is highly problematic since even a minute amount of dye can remain highly visible [3]. In recent studies, the low-cost chemically modified *Citrullus lanatus* peels were used for the sorption of lead (II) and cadmium (II) ions in batch studies from wastewater. It was concluded that base-modified adsorbents were more efficient [4]. Synthetic dyes are chemical substances which are frequently used in many industrial fields such as textile, leather, printing, cosmetic, pharmaceutical, food, paper, and wool industries. From the structural point of view, dyes may be acidic, basic, azo, diazo, reactive, disperse, and complexes of metals. From the literature, it is evaluated that more than 10^5 dyes are available commercially, and according to an estimate, 9×10^5 of dyes are synthesized every year [5]. Therefore, discharging of dyes containing wastewater into the water reservoirs causes serious water pollution which has adverse effects on mankind and aquatic life. In the modern world, water pollution is highly alarming due to the development of the above-mentioned industries which generate a huge amount of dye pollutants during processing [6]. It has been observed that in the whole world that the total dye consumption is about 10^4 tons/year and approximately 10 to 15% of these dyes are

discharged as effluents during dyeing processes [7]. Mostly, dyes such as brilliant green dye are aromatic in nature and easily biodegraded and release poisonous and carcinogenic products, which are harmful to humans and aquatic lives [8]. Dye effluents in wastewater affect the photosynthesis process of aquatic plants by depleting the dissolved oxygen and hindering the passage of sunlight into water bodies [9]. Based on industrial usage, generally, dyes are classified as anionic dyes (reactive dyes, acid dyes, and direct dyes) and cationic dyes (disperse dyes, nonionic dyes, and basic dyes). A toxic and carcinogenic brilliant green basic dye is extensively used in textile and printing industries. In this study, it is selected as a model dye for its adsorptive removal from wastewater [10]. Synthetic dyes such as vat dyes and disperse dyes are insoluble, while the remaining dyes are soluble in water [11]. Various conventional techniques for the removal of dye effluents from wastewater have been used, which may be biological, physical, or chemical [12]. Typical methods to treat colored water containing dye effluents have high operational and maintenance costs, so a low-profit industry cannot maintain it within its resources [13]. Hence, the treatment of industrial wastewaters containing dyes by adsorption on low-cost adsorbents is an emerging area of research and technology. Adsorption of dyes involves four major steps; first, dye particles diffuse through the solution, following further diffusion through an inner boundary layer and then into the interior of the adsorbents. Finally, molecular interactions (Van der Waals forces) bind the dye molecules on the surface of the adsorbents [14]. *Trapa natans* and *Citrullus lanatus* peels are the biosorbents selected in this research project for the detoxification of dye effluents released from industries into water bodies. The adsorption capacity for the removal of textile dyes has not been explored by chemical citric acid-modified adsorbents, which makes this a novel approach. The objectives of the present study are the utilization of *Trapa natans* and *Citrullus lanatus* peels as potential adsorbents for the removal of dyes from an aqueous solution and optimization of parameters such as temperature, pH, adsorbent dose, initial dye concentrations, and contact time. The adsorption models Langmuir, Freundlich, Temkin, pseudo-first order, and pseudo-second order will be used to check and explore the efficiency of novel chemically citric acid-modified adsorbents [15]. *Trapa natans* (water chestnut; water caltrop) belongs to family Trapaceae or Lythraceae [16], and *Citrullus lanatus* (watermelon) belongs to family Cucurbitaceae [17]. From the literature, the effect of operating parameters such as carbonization temperature and carbonization time on the adsorption phenomenon is studied [18]. It was also noted that *Citrullus lanatus* peels are composed of pectin, proteins, citruline, and carotenoids [19]. This study is significant for the adsorptive removal of brilliant green dye (BGD) from wastewater. It is a highly toxic cationic dye recently used in the fabric dyeing process and in printing industries [20]. Drinking water containing BGD has serious adverse effects on human health such as dermatitis and malfunctions of gastrointestinal and respiratory organs such as shortness of breath [21, 22]. The structure of brilliant green dye is shown in Figure 1.

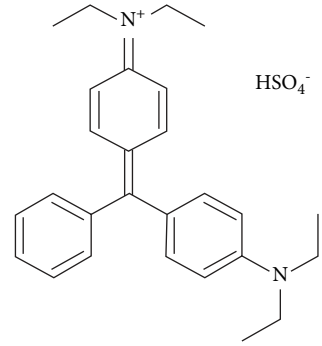

Figure 1: Structure of brilliant green dye [23].

The surface of both adsorbents, *Trapa natans* peels (TNPs) and *Citrullus lanatus* peels (CLPs), is composed of numerous functional groups, such as -COOH and -OH, which on deprotonation make their surfaces negatively charged. In this way, numerous negative adsorption sites on their surfaces are produced, which interact with BGD cationic molecules during adsorption in an aqueous solution. Citric acid, being a tricarboxylic acid chelating agent, enhanced the acidity of TNP and CLP, by providing additional carboxyl and hydroxyl groups. Therefore, citric acid-treated *Trapa natans* peels (CA-TNPs) and citric acid-modified *Citrullus lanatus* peels (CA-CLPs) have more adsorption capacity due to the deprotonation of these additional functional groups [24]. In this study, ecofriendly and inexpensive adsorbents are used for the eradication of brilliant green dye (BGD) from water.

2. Materials and Methods

2.1. Chemicals. The chemicals used are as follows: brilliant green dye ($\lambda_{max} = 625$ nm), HCl (11.6 M, 37%), sodium hydroxide (40 g/mol), potassium chloride (75.5 g/mol), sodium hydrogen carbonate (84 g/mol), sodium chloride (58 g/mol), phenolphthalein, iodine crystals (253.81 g/mol, 99.8%), methyl orange, potassium iodide (166 g/mol), sodium carbonate (58.5 g/mol), citric acid (192.12 g/mol), tartaric acid (150.087 g/mol), lactic acid (90 g/mol), urea (60 g/mol), thiourea (76 g/mol), EDTA, ethanol (46 g/mol), methanol (32 g/mol), isopropanol (60 g/mol), and acetone (58 g/mol). All glassware was washed with chromic acid and distilled water for the experiments. These were sterilized at 70°C for 0.5 hours in an electric oven. The other instruments used were an electrical grinder, measuring balance, pH meter, electric furnace, electric orbital shaker, and UV-visible spectrometer.

2.2. Preparation and Characterization of Adsorbents. *Trapa natans* peels (TNPs) and *Citrullus lanatus* peels (CLPs) were collected from different sites of the market in Lahore, Kasur, and Multan. These were washed subsequently with tap and distilled water and dried in sunlight. Then, these were placed in an oven at about 80°C for three days,

and afterward, the adsorbents were crushed and sieved through a 60-mesh sieve. The adsorbents were stored in plastic jars and labeled as TNP and CLP for further use during the experimental work [25]. These were characterized by physiochemical methods [26].

2.3. Selection of Chemicals for Chemical Processing of Adsorbents. Citric acid-treated peels of *Trapa natans* and *Citrullus lanatus* were used for the detoxification and removal of brilliant green dye (BGD) from aqueous solutions. Citric acid chemical-processed adsorbents showed better results of adsorption as compared to their raw forms during experimental work. Their efficiency was also compared with the previously reported adsorbents, elaborated in Table 1. Different chemicals (modifying agents) mentioned in Section 2.1 were also used for the chemical processing of adsorbents, but better results were obtained with citric acid-modified adsorbents (CA-TNP and CA-CLP). The chemical modification decreases the moisture content and increases the porosity and surface area of adsorbents [27]. The net charge on the surface of adsorbents was determined by the point of zero charge (pzc-pH) by acid-base titrations. If (pH > pzc-pH), then the adsorbent surface would be more negatively charged, and cations of basic dyes are readily attracted toward negatively charged adsorbent surfaces and vice versa [28, 29]. In this study, brilliant green dye (BGD) was selected due to its highly toxic nature and carcinogenic effects on humans and animals. It is a basic dye, and on dissolution in an aqueous solution, it provides cations (BGD^+). These adsorbents were also treated with different chemicals separately, such as ethanol, methanol, isopropanol, 0.1 M HCl, and 0.1 M NaOH, and some chelating agents such as urea [30], thiourea [31], EDTA [32], tartaric acid [33, 34], citric acid [35–37], lactic acid [38], and acetone [39]. Both adsorbents were chemically processed with organic solvents (ethanol, methanol, and isopropanol) for their modifications in glass beakers covered with aluminum sheets for a period of 3 to 4 hours. Excessive soaking of each adsorbent in these organic solvents was avoided to prevent their decline and deterioration, followed by the lumping of lignocellulosic materials. Then, these were filtered to get modified biosorbents. These were dried and added to 25 mL, 25 ppm solutions of BGD separately for 15 minutes at 100 rpm to determine the final concentration of the dye after the adsorption process [40]. For solid-phase chemical modification, selected modifying chelating agents and each biosorbent were taken in a ratio of 1 : 9 by mass in a china dish. These were mixed and irradiated with microwaves for an interval of nine (9) minutes each in a microwave oven.

The scheme is elaborated in Figures 2(a) and 2(b). The resulting chemically modified products were washed with distilled water and dried at 80°C. These were stored in plastic air-tight jars for further use in the research work. Figure 2(a) represents a schematic chemical treatment of both agro-wastes with different modifying chemical agents, while a schematic proposed structure of citric acid-modified adsorbents is shown in Figure 2(b).

2.4. Batch Studies for the Adsorption Process

2.4.1. Optimization of Parameters. The adsorption of BGD on R-TNP, CA-TNP, R-CLP, and CA-CLP depends on the chemical composition and available binding sites on the surface of adsorbents. To optimize the factors such as contact time, adsorbent dose, agitation speed, effect of the pH of the dye solution, temperature, and adsorption isothermal, kinetic studies were performed. The % age adsorption of BGD on each adsorbent was calculated by using the following equation:

$$\%\ \text{age adsorption of dye} = C_0 - \frac{C_e}{C_0} \times 100, \tag{1}$$

where C_0 (ppm) is the initial concentration of BGD (dye) and C_e (ppm) is the adsorption at equilibrium.

The quantity of dye (BGD) ($mg{\cdot}g^{-1}$) can be calculated from the following equation:

$$q = (C_0 - C_e) \times \frac{V}{m}, \tag{2}$$

where q ($mg{\cdot}g^{-1}$) is the amount of dye adsorbed by the adsorbent, V (L) is the volume of the BGD solution, and m (g) is the mass of the adsorbent [40, 57].

2.4.2. Biosorption Experiments. To optimize the adsorbent dose, raw adsorbents (R-TNP and R-CLP) and citric acid-modified adsorbents (CA-TNP and CA-CLP) ranging from 0.2 to 2.0 grams with a difference of 0.1 gram of each were added, in four (4) sets of ten 100 mL Erlenmeyer flasks. Each set of flasks contains 25 ppm with a volume of 25 mL of BGD solution. Repeated experiments were performed to optimize the other factors such as contact time (5 to 60 min) with a difference of 5 min each, agitation speed (25 to 200 rpm) with a difference of 25 rpm, temperature (10 to 80°C) with a difference of 10°C each, and pH (1 to 10).

3. Results and Discussion

3.1. Chemical Treatment of Adsorbents. From the comparative study, elaborated in Figure 3, it was noticed that the adsorption capacity of adsorbents (TNP and CLP) was significantly enhanced by using citric acid as a modifying agent, as discussed in Section 2.3. The novelty of this work is the chemical treatment of TNPs and CLPs with citric acid for better adsorptive removal of basic dyes (BGD) due to its chelating effect and deprotonation in aqueous media. Being a tricarboxylic acid, citric acid is an excellent chelating agent and creates more interactions due to esterification with adsorbents than other acids such as tartaric acid, lactic acid, and HCl [58]. It is interesting to note that rapid adsorption equilibrium was established by chemically modified adsorbents during the experimental work [59]. Therefore, it favors the removal of BGD cations by esterification from an aqueous solution. Figure 3 revealed that citric acid chemical-treated biosorbents showed more efficient adsorption results than other modifying agents. The solid-phase chemical

Table 1: A comparative study of adsorption with some previously reported biosorbents for the biosorptive removal of brilliant green dye.

Reported biosorbents	q_{max} (mg/g)	References
Rambutan peels	9.64	[41]
Jackfruit peels	6.12	[41]
Almond peels (acid processed)	30	[42]
Cempedak durian peel	97.99	[43]
Salix alba leaves	8.47	[44]
Snail shell and rice husk	131.1	[45]
NaOH-modified walnut shell	146.4	[46]
Nephelium mutabile leaves	130.3	[47]
Peganum harmala activated carbon	35.97	[48]
Na_2CO_3-treated *Bambusa tulda*	41.67	[49]
The sponge of *Luffa cylindrical*	18.52	[50]
Raw beech sawdust	51.28	[51]
Binary oxidized cactus fruit peel	166.66	[52]
Activated carbon from acorn	2.11	[53]
Chemically treated *Lawsonia inermis* seed powder	34.96	[54]
Physically and chemically activated carbon from *Araucaria angustifolia*	298.5	[55]
Native watermelon rind (WR)	92.6	[56]
H_3PO_4-treated activated (AWR) watermelon rind	188.6	[56]
Raw *Trapa natans* peels	108.69	This study
Citric acid-modified *Trapa natans* peels	128.30	This study
Raw *Citrullus lanatus* peels	144.92	This study
Citric acid-*modified Citrullus lanatus* peels	188.68	This study

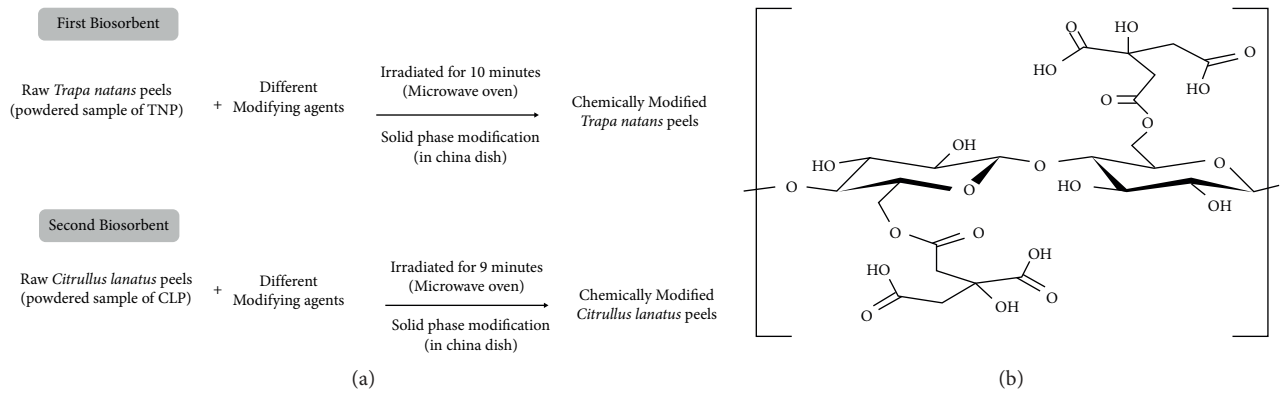

Figure 2: (a) Scheme of chemical modification of peels. (b) Scheme of chemical-modified adsorbent (CA-TNP and CA-CLP).

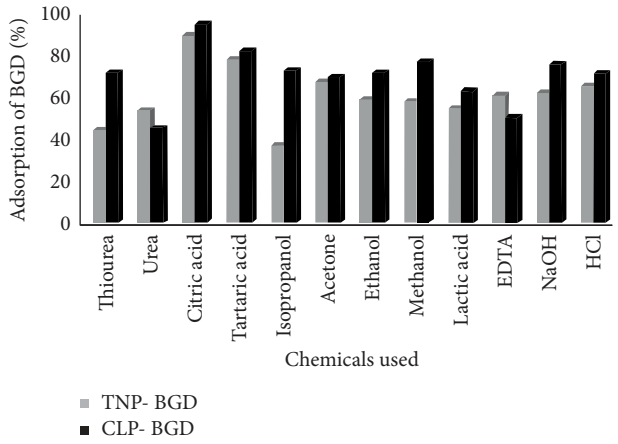

Figure 3: Comparative adsorption behavior of TNP and CLP after modification with different chemicals.

modification of adsorbents (TNP and CLP) with chemicals such as urea, thiourea, tartaric acid, citric acid, and lactic acid was carried out under microwave radiation [24].

The previously reported literature also revealed that these chemically modified biosorbents gave better results of adsorption mechanism [60, 61]. The novel citric acid-modified *Trapa natans* and *Citrullus lanatus* peels were labeled as CA-TNP and CA-CLP, respectively.

3.2. Physicochemical Interpretation of Biosorbents. The physicochemical examination of the TNP and CLP is summarized in Table 2. Adsorbents were characterized by different techniques such as Boehm titration to determine the nature of sites which may be acidic or basic, iodine titration, calculation of porosity/bulk density, moisture content, ash content, volatile matters, and pH, and elemental analysis [26].

3.3. FTIR Analysis of Adsorbents. The FTIR spectra of both adsorbents before and after chemical treatment with citric acid are shown in Figure 4 and for the adsorption of BGD on raw adsorbents (R-TNP and R-CLP) and chemically modified adsorbents (CA-TNP and CA-CLP) are shown in Figure 5. For spectroscopic analysis, 0.6 g of each adsorbent (R-TNP, CA-TNP, R-CLP, and CA-CLP) was added to a 25 mL solution of brilliant green dye (BGD) having concentration 25 ppm. These were agitated at 100 rpm for 25 minutes at 25°C in Erlenmeyer flasks. After filtration, the residues were washed with distilled water and evaporated to perform FTIR [62]. The FTIR spectra before and after the adsorption of BGD on unmodified (R-TNP and R-CLP) and chemically modified (CA-TNP and CA-CLP) adsorbents are shown in Figures 4 and 5, respectively.

In Figure 4(a), the spectrum of unmodified TNP is shown, where the strong band at 3250 cm^{-1} represents the O-H (stretching) for carboxylic acids and at 2870 cm^{-1} indicates the C-H (stretching) for alkanes. The peaks at 2367 cm^{-1} represent the adsorbed atmospheric carbon dioxide molecules. The frequency at 1430 cm^{-1} is a sign of O-H (bending) for carboxylic acid functional groups. The medium peak at 1339 cm^{-1} shows the O-H (bending) for phenol. Figure 4(b) shows the citric acid-treated TNP spectrum, which represents the new sharp peaks between wavenumbers 3850 and3600 cm^{-1}, for the esterification reaction between COOH groups of tricarboxylic citric acid and free O-H groups of the lignocellulosic surface of TNP. A modified peak at 2930 cm^{-1} indicates the C-H (stretching) for alkanes, while the region between 2200 and 2100 cm^{-1} represents the stretching groups of alkynes. A comparison of both spectra indicates the variations in citric acid-treated TNP compared to its raw form (R-TNP). Figure 4(c) represents the FTIR spectrum of R-CLP, in which medium peaks at 3770 to 3414 cm^{-1} are signs of free O-H (stretching) groups for alcohols while two strong peaks at 2960 and 2860 cm^{-1} represent the N-H (stretching) for amine groups. A weak band at 2100 cm^{-1} shows the presence of stretching groups for alkynes and at 1638 cm^{-1} for (stretching) alkenes. The frequency of the strong peak at 1330 cm^{-1} indicates the presence of C-N (stretching) for aromatic amines. Figure 4(d) represents the spectrum of citric acid-modified CLP, which is obviously different from the spectrum of R-CLP shown in Figure 4(c). A number of new peaks obtained between regions 3870 and 3730 cm^{-1} evidenced the esterification reaction between COOH groups of citric acid and free OH groups on the surface of the raw CLP adsorbent.

The medium peaks at 2940 and 2870 cm^{-1} are signs of the C-H (stretching) of alkanes. The peak at 2330 cm^{-1} represents the atmospheric CO_2, while the 2120 cm^{-1} frequency shows the monosubstituted alkynes. From the above-mentioned study, it was concluded that citric acid-treated adsorbents CA-TNP and CA-CLP are different in surface morphology from their raw and untreated forms due to the reaction between acid and lignocellulosic materials of biosorbents.

FTIR spectra for adsorption of BGD on untreated and chemically citric acid-treated adsorbents are shown in Figure 5. In Figure 5(a), a few peaks ranging from 3860 to 3600 and at 3270 cm^{-1} indicate the interactions between BGD and free O-H groups on the surface of R-TNP. The strong broad bands at 2950 and 2822 cm^{-1} represent the N-H (stretching) for amines. A medium peak at 1617 cm^{-1} indicates the C=C (stretching) for conjugated alkene and at 1437 cm^{-1} indicates O-H (bending) for carboxylic acid. A strong broad peak at 1022 cm^{-1} shows the C-N (stretching) group for primary amines. In Figure 5(b), the additional peaks ranging from 3925 to 3600 cm^{-1} are associated with intermolecular hydrogen bonding between additional esterified carboxylic acid moieties on the surface of CA-TNP. The decrease in wavenumber from 2950 to 2917 cm^{-1} is associated with the efficient adsorption of BGD on CA-TNP compared with R-TNP. Weak peaks at 2200 cm^{-1} represent the presence of stretching disubstituted alkynes, and regions between 1680 and 1636 cm^{-1} represent the associations of C=O secondary amide with BGD molecules, while a strong, unchanged, broad peak at 1022 cm^{-1} was observed for the C-N (stretching) group of primary amines. In Figure 5(c), wave number ranging from 3900 to 3722 cm^{-1} is evidenced for free O-H association with BGD molecules on the surface of lignocellulosic materials of CLP, while strong and broad peaks at 2915 and 2848 cm^{-1}, as compared to R-CLP in Figure 4(c), indicate the associations of N-H groups for amines with BGD molecules. The peaks ranging from 1465 to 1450 cm^{-1} represent the C-H (bending) for methyl groups of alkanes. The change in the band from 1330 cm^{-1} (Figure 4(c)) to 1374 cm^{-1} shows the adsorption of BGD due to O-H groups for phenol. A strong, broad peak at 1022 cm^{-1} shows the C-N (stretching) group for primary amines. Comparing Figure 5(c) with Figure 5(d), the consecutive increase in the number of peaks from 3833 to 3740 cm^{-1} is evidence of the good adsorption of BGD on CA-CLP, due to the availability of more esterified -COOH functional groups of citric acid. The oxygen containing functional groups on lignocellulosic materials facilitate the adsorption of cationic dyes such as BGD [63]. A broad, strong peak at 3400 cm^{-1} indicates the intermolecular bonding of BGD due to O-H (stretching) groups of alcohols on the surface of CA-CLP. The decrease in peaks at 2917 and 2850 cm^{-1} in Figure 5(d),

Table 2: Physicochemical analysis of adsorbents [16].

Factors		Values of TNP		Values of CLP
Moisture %		8		7.9
pH		5.8		5.1
Particle density (g/cm^3)		0.60		0.48
Bulk density p_{wet}		0.516		0.953
Porosity %		0.8		0.153
Ash content %		7		2.1
Volatile matter content %		93		4.71
Iodine number (mg/g)		15.5		2.1
Carboxylic acidic functional groups (m·mol)		0.035		1.9973
Basic sites (m·mol)		0.005		1.99
Phenolic groups (m·mol)		0.08		0.004
Lactones (m·mol)		0.06		0.006
Element contents (mg/kg)	Cd(II)	0.629	Mn(II)	14.2
	Ni(II)	0.557	P	1352.4
	Zn(II)	0.371	Zn(II)	12.9
	Mg(II)	0.213	Mg(II)	14.8
	Ca(II)	0.171	Ca(II)	291.5
	K(I)	0.22	K(I)	13.7
	Na(I)	0.19	Na(I)	12.9

as compared to Figure 5(c), is a sign for good adsorption of BGD on citric acid-treated CLP. The peaks ranging between 1760 and 1755 cm^{-1} indicate the interactions of BGD with C=O (stretching) for carboxylic acid monomers on CA-CLP. The peaks ranging from 1540 to 1500 cm^{-1} indicate the N-O (stretching) nitro groups, while the wavenumbers ranging from 1437 to 1350 cm^{-1} evidenced the interactions of BGD on CA-CLP due to O-H (bending) of carboxylic acid groups. A strong, broad peak at 1022 cm^{-1} shows the C-N (stretching) group for primary amines. It is evidenced from the abovementioned comparative study of FTIR spectra that citric acid-treated novel adsorbents, CA-TNP and CA-CLP, have better adsorption capacity than their untreated raw forms, R-TNP and R-CLP.

3.4. SEM Micrograph Study. For the morphological study, SEM micrographs of unmodified adsorbents [64, 65] (R-TNP, R-CLP) and citric acid-modified adsorbents (CA-TNP, CA-CLP) were taken.

In Figure 6(a), R-TNP showed the compact arrangement of cylindrical structures having crevices, voids, and interstices, but in its citric acid chemically modified form (CA-TNP), represented in Figure 6(b), the body structures are converted into flaky with cages and wavy fibers, resulting in increased binding sites, surface area, and also, space for the adsorption of BGD. Figure 6(c) elaborates the structural chemistry of R-CLP and shows the voids and interstices between the numerous round bodies and compact spherical structures, but its chemical modification with citric acid, shown in Figure 6(d), converted it into fluffy, flakey, and wavy bodies with a number of potential binding sites for BGD adsorption. A cluster of citric acid moieties seen well on the surface of the chemically modified novel adsorbent CA-CLP evidenced numerous active binding sites for good and enhanced adsorption. Citric acid breaks and decreases the cellulose crystallinity of lignocellulosic biomass, resulting in increased porosity and surface area of TNP and CLP [66]. Total emplacement sites on the biosorbent surface can be increased by providing additional functional groups during the chemical treatment with suitable modifying agents [67, 68]. Thus, the surface of adsorbents favors more electrostatic and hydrogen bonding interactions with the cationic molecules of BGD due to the presence of a lot of negatively active binding sites.

3.5. Optimization of Parameters. Optimum conditions for the adsorption of BGD on R-TNP, R-CLP, CA-TNP, and CA-CLP were determined by studying the various factors and parameters such as temperature, pH, adsorption dose, contact time, and agitation speed [69].

3.5.1. Effect of Adsorbent Dose on Adsorption. For the adsorption mechanism, the amount of adsorbent dose has a significant role. The high concentration of dye readily establishes the equilibrium with adsorbents and leaves many vacant adsorption sites, resulting in less removal of BGD from aqueous media. Citric acid acts as a chelating agent in CA-TNP and CA-CLP, increasing the active binding sites for more adsorption processes [59]. Hence, it was noted that BGD adsorption efficiency increases with a lower dose of adsorbent. At 30°C and 100 rpm, the optimum adsorption percentage of BGD was 73.6% on 1.4 g of R-TNP, 82% on 1.2 g of R-CLP, 96.8% on 0.8 g of CA-TNP, and 98.9% on 0.8 g of CA-CLP recorded as shown in Figure 7.

3.5.2. Effect of Contact Time Intervals. Contact time duration is the major factor necessary to determine the rate of adsorption of dye on the biosorbent. Active binding sites on the biosorbent, dyestuff (cationic or anionic), and interactions between adsorbate and adsorbents determine the efficiency and rate of adsorption. With the increase in time,

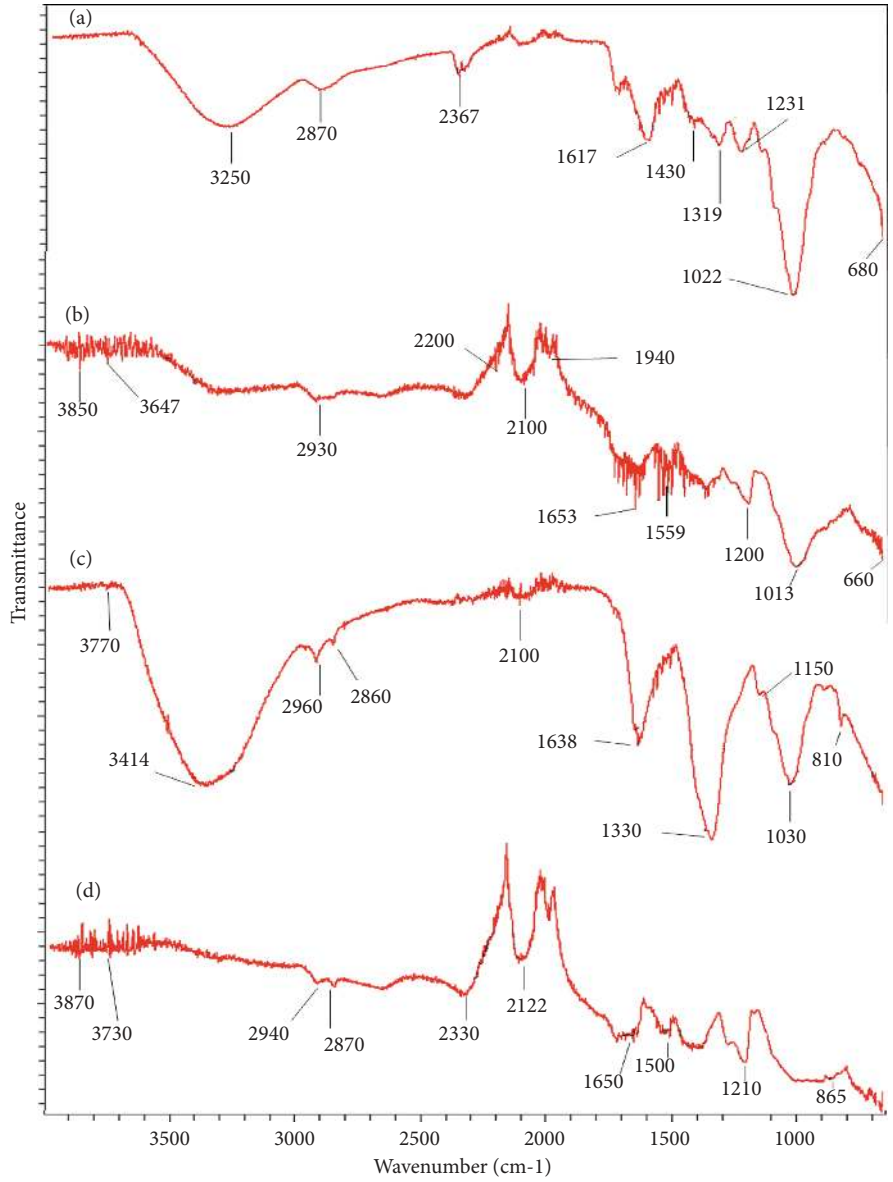

Figure 4: FTIR spectra of untreated and citric acid-treated peels before the adsorption of dye (BGD). (a) R-TNP, (b) CA-TNP, (c) R-CLP, and (d) CA-CLP.

the saturation of the adsorbate (BGD) on the biosorbent increases. As a result, equilibrium is established and the adsorption decreases [70]. Citric acid-modified biosorbents (CA-TNP and CA-CLP) have more active binding sites; hence, adsorption occurs more readily than unmodified biosorbents (R-TNP and R-CLP). However, with the passage of time, the dyestuffs accumulate on the biosorbents and decrease the rate of adsorption [71]. 0.6 g of each biosorbents (R-TNP, R-CLP, CA-TNP, and CA-CLP) was added in four (4) sets of twelve 100 mL Erlenmeyer flasks. Each set of flasks contains 25 ppm with a volume of 25 mL of BGD solution at pH 6 and 100 rpm agitation speed. R-TNP removed 68% BGD at 45 minutes, whereas citric acid-modified biosorbent CA-TNP detoxified 92.6% BGD in a 25-minute time interval. The second biosorbent, R-CLP, removed 82% BGD at 35 minutes, whereas the citric acid-modified biosorbent, CA-CLP, showed high efficiency by removing 96.8% BGD in a 20-minute time interval, elaborated in Figure 8.

3.5.3. Effect of Agitation Speed on Adsorption. It is another important factor that impacts the dye removal from aqueous solutions during the adsorption mechanism. It was observed that high rotating speed was directly related to the adsorption phenomenon due to the formation of a thin film of dye molecules from the bulk of solute (BGD). This unique external boundary of dye molecules ultimately enhanced the adsorption phenomenon. In this study, the maximum detoxification of BGD was achieved at 95.7% at 100 rpm using 0.8 g of CA-CLP and 85% at 125 rpm for R-CLP, while the adsorption of BGD was 93.6% at 100 rpm for CA-TNP and 85% at 125 rpm for R-TNP. This factor was studied using

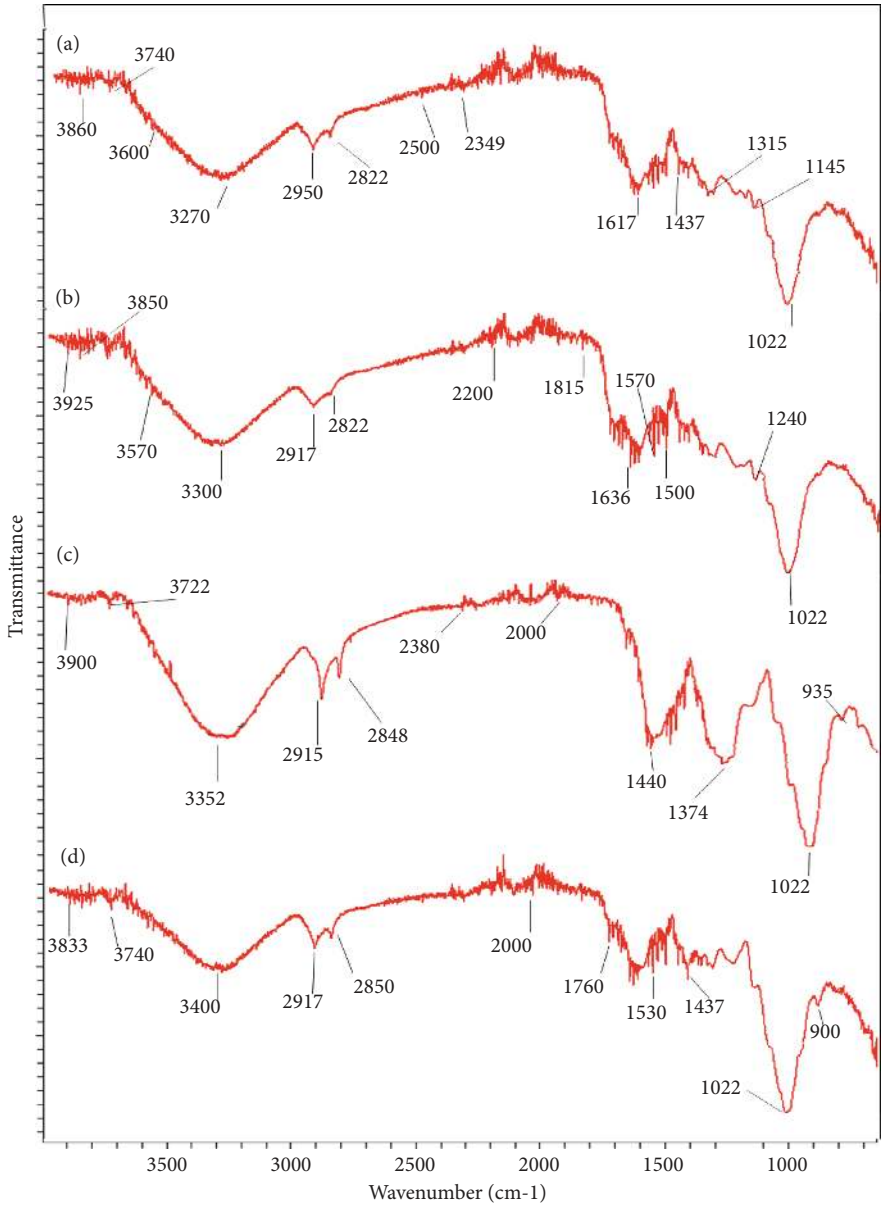

Figure 5: FTIR spectra of untreated and citric acid-treated peels after the adsorption of dye (BGD). (a) BGD-R-TNP, (b) BGD-CA-TNP, (c) BGD-R-CLP, and (d) BGD-CA-CLP.

0.8 g of each adsorbent in 4 sets of eight 100 mL Erlenmeyer flasks. Each set of flasks contains 25 ppm with a volume of 25 mL of BGD solution at pH 5 and 25 minutes' contact time, elaborated in Figure 9. At higher speed, the adsorption decreases due to the generation of overabundance centripetal power of free BGD molecules in the aqueous media. With further increase in centripetal force due to high speed, an effect of repulsion force is created on the adsorbed dye molecules on the binding sites of adsorbents, resulting in the desorption of the dye [72], as shown in Figure 9.

3.5.4. Effect of Temperature on Adsorption. Temperature affects the adsorption mechanism in an exothermic or endothermic way. Change in temperature is associated with change in the kinetic energy of molecules of BGD as well as the thermodynamics of the adsorption mechanism [73]. It was observed from the literature that the adsorption phenomenon is usually exothermic and, thus, a rise in temperature decreases the rate of adsorption [74]. In Figure 10, the results of the change in temperature from 10 to 80°C are reflected. The unmodified R-TNP removed 73.6% of BGD at 50°C, whereas the citric acid-modified adsorbent CA-TNP detoxified 90.5% of BGD at 30°C. The R-CLP removed 81% of BGD at 40°C, whereas the citric acid-modified adsorbent CA-CLP showed high efficiency of removal at 94.7% BGD at 30°C. It was noted that high temperature damages the structure of the adsorbent, resulting in swelling up and allowing more penetration of dye molecules inside of it [75]. Therefore, in this study, due to this reason, the adsorption in

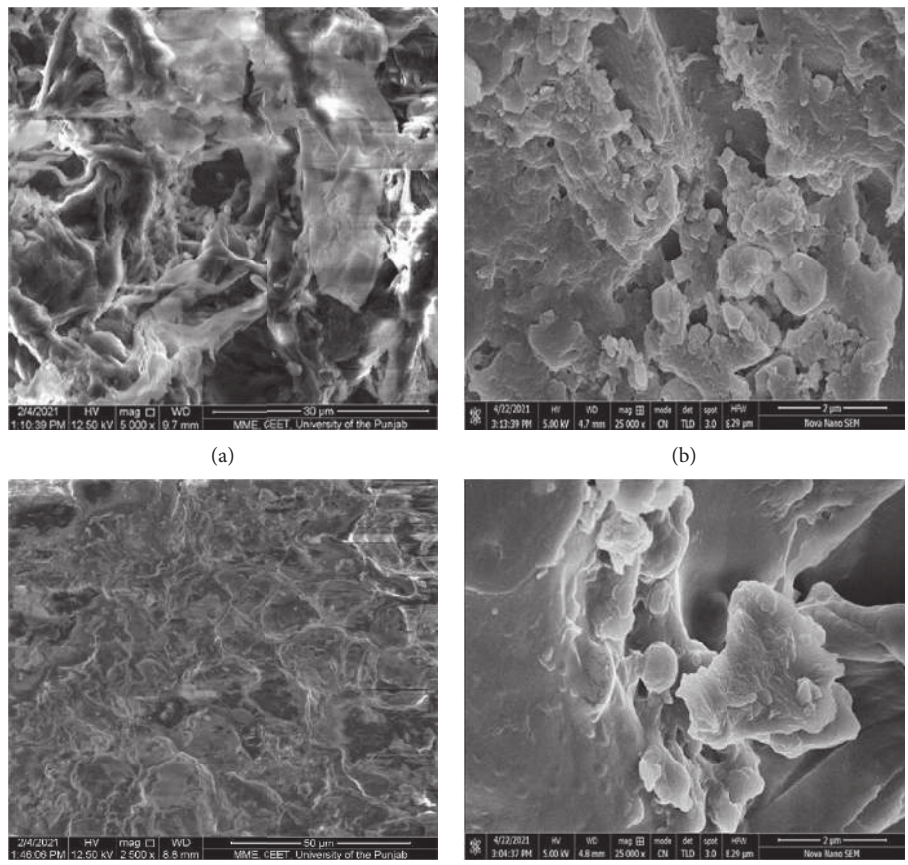

Figure 6: SEM of (a) R-TNP, (b) CA-TNP, (c) CLP, and (d) CA-CLP.

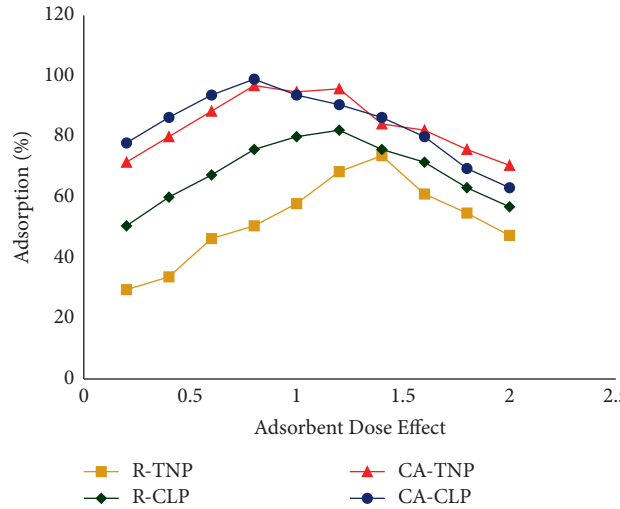

Figure 7: Effect of adsorbent dose on adsorption. Experimental conditions: adsorbent dose range 0.2 to 2.0 g, conc. = 25 ppm, volume = 25 mL, temperature 30°C, initial pH = 5, final pH: R-TNP = 5, R-CLP = 4.5, CA-TNP = 4.0, and CA-CLP = 4.0, contact time = 30 min, and agitation speed = 100 rpm.

some cases increases in high temperature ranges; e.g., in R-TNP, the adsorption increases from 60 to 70°C (61% to 65%), while in *R*-CLP, the adsorption increases from 50 to 60°C (77.9% to 80%), as expressed in Figure 10. On the other hand, heating above 50°C adversely affects the inhibitory properties of BGD, such as its loss of antimicrobial activity, associated with decolorization at high temperature [76]. A rise in temperature during the adsorption mechanism affects

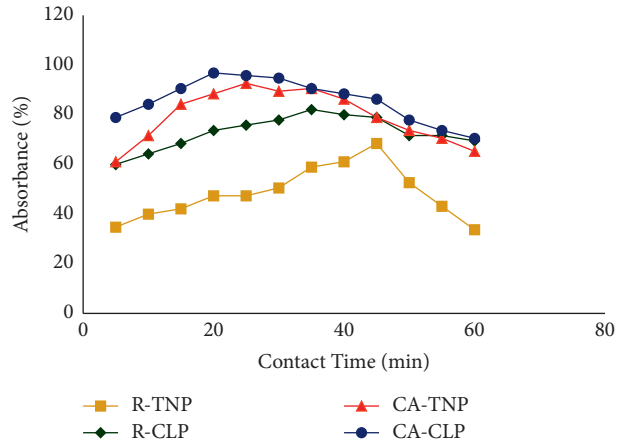

Figure 8: Effect of contact time on adsorption. Experimental conditions: contact time 5 to 60 min, conc. = 25 ppm, volume = 25 mL, temperature = 30°C, initial pH = 5, final pH: R-TNP = 5, R-CLP = 4.5, CA-TNP = 4.0, and CA-CLP = 4.0, adsorbent dose = 0.6 g, and agitation speed = 100 rpm.

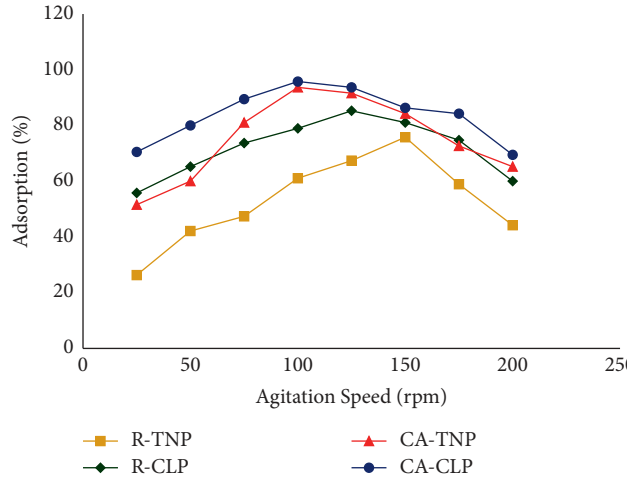

Figure 9: Effect of agitation on adsorption. Experimental conditions: agitation speed range 25 to 200 rpm, conc. = 25 ppm, volume = 25 mL, adsorbent dose = 0.6 g, contact time = 30 min, temperature 30°C, initial pH = 5, and final pH: R-TNP = 5, R-CLP = 4.5, CA-TNP = 4.0, and CA-CLP = 4.0.

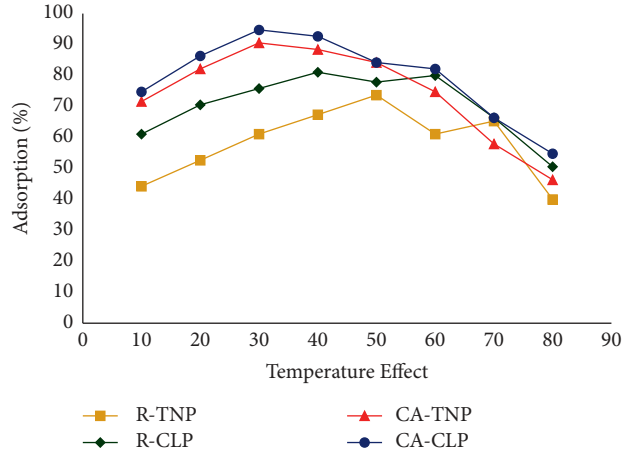

Figure 10: Effect of temperature on adsorption. Experimental conditions: temperature range 10 to 80°C, conc. = 25 ppm, volume = 25 mL, adsorbent dose = 0.6 g, contact time = 30 min, initial pH = 5, final pH: R-TNP = 5, R-CLP = 4.5, CA-TNP = 4.0, and CA-CLP = 4.0, and agitation speed 100 rpm.

the concentration of the solution due to evaporation of water from it. During the experimental studies, the flasks were covered with aluminum foil; thus, this effect was negligible.

3.5.5. Effect of pH on Adsorption. The impact of pH in the range from 1 to 10 was monitored as shown in Figure 11. The R-TNP removed 71.5% of BGD (before adsorption at pH = 7 and after adsorption at pH = 6), while the CA-TNP detoxified 92.6% of BGD (before adsorption at pH = 5 and after adsorption at pH = 4). Similarly, the second native adsorbent, R-CLP, removed 84% of BGD (before adsorption at pH = 6 and after adsorption at pH = 5), and its modified form, CA-CLP, showed high efficiency by removing 98% of BGD (before adsorption at pH = 5 and after adsorption at pH = 4.5). Both CA-TNP and CA-CLP at pH 5 showed better adsorption due to chelation between [BGD^+] and (COO^-) moieties of esterified tricarboxylic citric acid with the surface of TNP and CLP [77]. Raw adsorbents (R-TNP and R-CLP) showed the maximum adsorption at pH 7 and 6, respectively, due to the deprotonation of COOH groups, resulting in more negative adsorption sites on native adsorbents being produced for the adsorbate-adsorbent electrostatic associations. At high pH, during the equilibrium state, the excess [OH^-] ions were held with the remaining [BGD^+] ions in the solution through electrostatic forces and appear in the form of pairs. This action decreases the adsorption of adsorbate cations, at high pH values [78, 79]. It was also observed during the experimental study that, at low pH, the surface of biosorbents becomes more positively charged due to the protonation of adsorption sites. The resulting excessive (H^+) ions at the interface of adsorbate-adsorbent repel the [BGD^+] ions to access the adsorption binding moieties (COOH) [80]. This phenomenon decreased the removal of BGD from the aqueous solution, as expressed in Figure 11. On the other hand, an increase in pH decreases the concentration of (H^+) ions in the solution. This process favors the more adsorption of [BGD^+] ions on negative adsorption sites ($COO^{\rightarrow}$) of adsorbents with strong electrostatic interactions [9]. Thus, pH is an important factor. It was adjusted by adding 0.1 M NaOH or 0.1 M HCl solution for better adsorption during the experimental approach [81]. The point of zero charge (pH-PZC) of R-TNP and R-CLP is the point of isoelectronic, where the positive and negative charges of the adsorbent surface become equal [82, 83]. The pH-PZC value for native *Trapa natans* peels was 5.8 [84], while for native *Citrullus lanatus* peels, it was 5.6 [85]. If pH < pH-PZC, then the adsorbent surface is positively charged and repels the cationic dye molecules, whereas if pH > pH-PZC, then the surface of adsorbents is likely to be negatively charged due to deprotonation of functional groups such as -OH and -COOH and repels the anionic dye adsorption [84, 86].

3.6. Mathematical Modeling

3.6.1. Equilibrium Isothermal Studies. From isothermal studies, the data were correlated and studied under three mathematical models: Langmuir, Freundlich, and Temkin models. These are expressed in equations (3), (6), and (7), respectively. The optimized conditions for further study are mentioned below.

Adsorbent dose = 0.8 g, contact time = 25 min, temperature = 40°C, agitation speed = 100 rpm, pH = 5, and initial volume of solution V = 100 mL.

(i) Langmuir Isotherm:

The linear form of the Langmuir isothermal model is represented in equation (3), while graphically effective parameters are shown in Figure 12.

$$\frac{1}{q_e} = \left(\frac{1}{bq_{\max}}\right)\frac{1}{C_e} + \left(\frac{1}{q_{\max}}\right), \tag{3}$$

where q_e is the amount of dye adsorbed, C_e is the remaining amount of dye in ppm after adsorption, and q_m is in $mg{\cdot}g^{-1}$ while "b" is in $L{\cdot}g^{-1}$ [87].

Gibbs free energy change (ΔG^0) was calculated from the following equation:

$$\Delta G^0 = -RT \ln K, \tag{4}$$

where "R" is the universal constant ($8.3145\ J{\cdot}mol^{-1}k^{-1}$) and "$K$" is the inverse of Langmuir constant b.

Figure 12 shows the comparative study of the Langmuir isothermal model for the adsorption of BGD on unmodified adsorbents (R-TNP and R-CLP) and chemically modified with citric acid adsorbents (CA-TNP and CA-CLP), whereas the effective parameters for the Langmuir isothermal model are elaborated in Table 3. The correlation coefficient (R^2) for the adsorption of BGD on R-TNP, CA-TNP, R-CLP, and CA-CLP is 0.9858, 0.9863, 0.9853, and 0.9982, respectively. The $q_{\max}$ ($mg{\cdot}g^{-1}$) values for R-TNP, CA-TNP, R-CLP, and CA-CLP are 108.69, 128, 144.9, and 188.68, respectively, indicating that this model explains the adsorption of BGD in a better way for citric acid-modified adsorbents (CA-TNP and CA-CLP) than native adsorbents (R-TNP and R-CLP), as given in Table 3. By applying the relationship shown in equation (2), the separation factor (R_L) was calculated using a C value equal to 30 ppm. The values of $R_L < 1$ also favor the adsorption phenomenon according to the Langmuir isothermal model [88]. Comparison of q_m values showed better adsorption by the citric acid-modified adsorbents (CA-TNP and CA-CLP) than unmodified adsorbents (R-TNP and R-CLP). This leads to the novelty of this study.

$$R_L = \frac{1}{(1 + bC_0)}. \tag{5}$$

Furthermore, q_m values of all modified and unmodified adsorbents indicate a homogeneous monolayer adsorption mechanism on the fixed number of equivalent binding sites distributed on the surface of adsorbents [89].

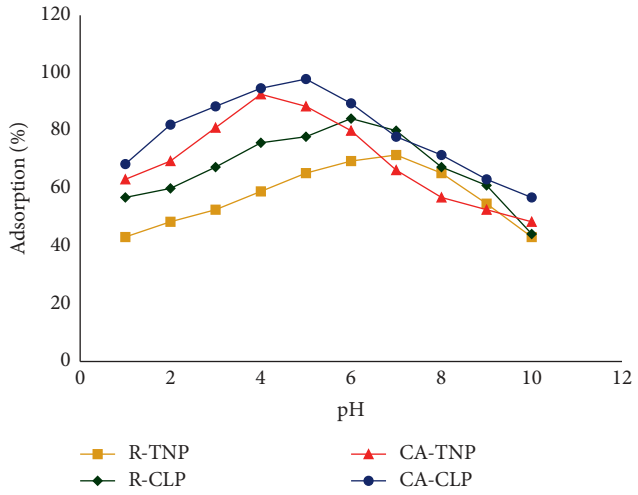

Figure 11: Effect of pH on the adsorption process. Experimental conditions: pH range 1 to 10, conc. = 25 ppm, volume = 25 mL, adsorbent dose = 0.6 g, contact time = 30 min, temperature 30°C, and agitation speed = 100 rpm.

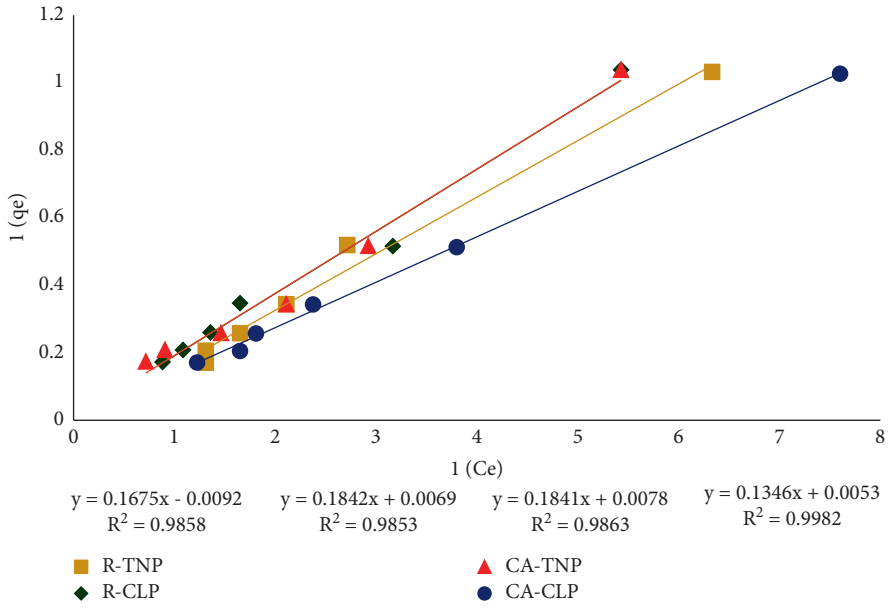

Figure 12: Comparison of the Langmuir isothermal effective parameter for the adsorption of BGD. Adsorbent dose = 0.5 g, contact time = 25 min, temperature = 30°C, agitation speed = 100 rpm, initial pH = 5, final pH: R-TNP = 5, R-CLP = 4.5, CA-TNP = 4.0, and CA-CLP = 4.0, and dye solution volume V = 100 mL.

(ii) Freundlich Isotherm:

The linear form of this isothermal model is represented in the following equation:

$$\log q = \log K_F + \frac{1}{n}\log C_e, \tag{6}$$

where "K_F"($mg^{1-1/n}{\cdot}L^{1/n}{\cdot}g^{-1}$) is the binding constant related to the adsorption capacity and "n" is the adsorption intensity [90]. The surface heterogeneity or the adsorption capacity can be measured from $1/n$ which ranges from 0 to 1. The lowest value of $1/n$ indicates the presence of more heterogeneity and multilayer adsorption [91]. Figure 13, elaborates the Freundlich isothermal plot ($\log q_e$ vs. $\log C_e$) for the adsorption of BGD on unmodified (R-TNP and R-CLP) and chemically modified with citric acid (CA-TNP and CA-CLP) adsorbents. This plot gives straight lines of all (R-TNP, R-CLP, CA-TNP, and CA-CLP) adsorbents, with slope $1/n$, ranging from 0 to 1. Correlation coefficient (R^2) values for the adsorption of BGD on the adsorbent active sites of R-TNP, CA-TNP, R-CLP, and CA-CLP are 0.9405, 0.9871, 0.9867, and 0.9433, respectively. This can also be analyzed from Figure 13.

A comparison study of both of these isothermal models in Table 3 shows that the Langmuir isothermal model fits better than the Freundlich isotherm model. From FTIR analysis, citric acid-

Table 3: A comparative study of isothermal parameters for the detoxification of BGD.

Adsorption model	R-TNP	CA-TNP (acid treated)	R-CLP	CA-CLP (acid treated)
		Langmuir isotherm		
R^2	0.9858	0.9863	0.9853	0.9982
q_{max} (mg·g^{-1})	108.69	128.2	144.92	188.68
R_L (L·mg^{-1})	0.3777	0.440	0.471	0.458
b (L·mg^{-1})	0.0549	0.0423	0.0374	0.0394
RMSE	11.462	11.71	11.603	13.795
		Freundlich isotherm		
R^2	0.9405	0.9871	0.9867	0.9433
$1/N$	0.852	0.766	0.951	0.922
n (1/m)	1.1730	1.3044	1.0506	1.0844
K_f (mg·g^{-1})	5.917	4.712	5.113	6.579
RMSE	11.644	11.777	11.989	14.169
		Temkin isotherm		
R^2	0.982	0.987	0.970	0.991
B_T (J·mol^{-1})	2.307	2.345	2.298	2.315
A_T (L·g^{-1})	7.280	7.458	7.412	7.705

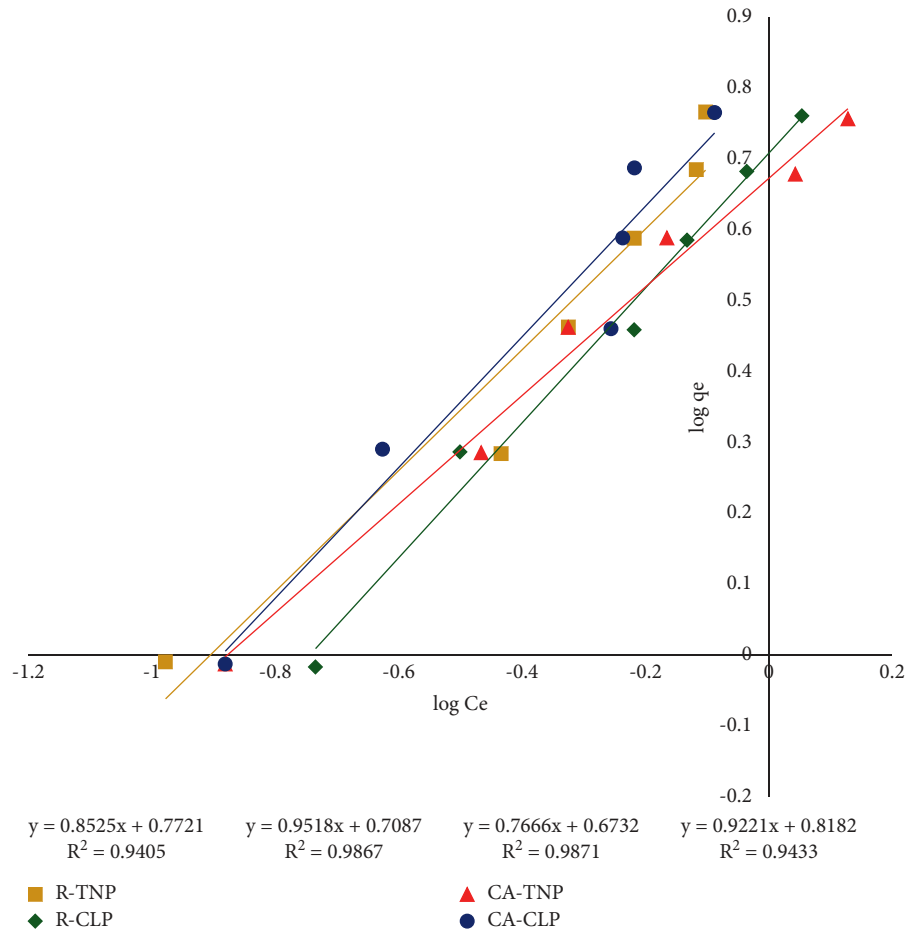

Figure 13: Comparison of effective parameters of Freundlich isotherm for the adsorption of BGD. Adsorbent dose = 0.5 g, contact time = 25 min, temperature = 30°C, agitation speed = 100 rpm, initial pH = 5, final pH: R-TNP = 5, R-CLP = 4.5, CA-TNP = 4.0, and CA-CLP = 4.0, and dye solution volume V = 100 mL.

modified adsorbents, CA-TNP and CA-CLP, have more active binding sites for the adsorption of BGD than their native adsorbents, R-TNP and R-CLP.

(iii) Temkin Isotherm:

The basic assumption of this isothermal model is that the heat of adsorption of adsorbate (BGD molecules) on the surface of adsorbents (R-TNP, CA-TNP, R-CLP, and CA-CLP) linearly decreases with the increase in coverage of their surfaces by dye molecules [92]. The linear form of the Temkin isothermal model is represented in equation (7) and graphically in Figure 14.

$$q_e = B_T \ln C_e + B_T \ln A_T, \tag{7}$$

where $B_T = (RT/b_T)$ (kj·mol^{-1}) is the Temkin isotherm constant which indicates the heat of adsorption during the adsorption phenomenon, while "A_T" (L·g^{-1}) represents the equilibrium binding constant which gives information about the maximum binding energy [93].

The abovementioned constants in this study were obtained by the comparative study of the regression analysis of linear plots of the unmodified (R-TNP and R-CLP) and citric acid-modified (CA-TNP and CA-CLP) adsorbents between "q_e" and lnC_e, elaborated in Figure 14. The Temkin equilibrium model of isotherm anticipated an equivalent distribution of binding energies on the surface of adsorbents due to the number of dynamic binding sites [94, 95]. The heat of adsorption (B_T) is used to determine the interactions between the adsorbate and adsorbent. $B_T < 8$ kj·mol^{-1} indicates weak and physical binding forces, while $B_T > 8$ kj·mol^{-1} reveals strong and chemical interactions between the adsorbate and adsorbent [96, 97]. From Table 3, it can be seen that the heat of adsorption (B_T) for the adsorption of BGD on unmodified adsorbents, R-TNP and R-CLP, is 2.3076 and 2.2981, respectively, whereas for novel citric acid-modified adsorbents, CA-TNP and CA-CLP, it is 2.3448 and 2.3146, respectively, which when less than 8 depict the weak binding forces, which are physical in nature.

The temkin isotherm constant (B_T) reflects that citric acid-modified novel adsorbents offer more binding forces for BGD molecules than unmodified ones. The correlation coefficients (R^2) for the Temkin model for novel modified adsorbents are more than those for unmodified adsorbents. Hence, this model is also the best fit, like the Langmuir isotherm shown in Table 3. These parameters indicate the physisorption instead of chemisorption and heterogeneity [98].

Nonlinear equations (8)–(10) of the linear modes of Langmuir, Freundlich, and Temkin isotherms, respectively, are given below [99].

$$q_e = \left[\frac{b \cdot q_{\max} \cdot C_e}{(1+b) \cdot C_e}\right], \tag{8}$$

$$q_e = \left[K_F \cdot C_e^{1/n}\right], \tag{9}$$

$$q_e = B_T \ln\left(A_T \cdot C_e\right). \tag{10}$$

The abovementioned nonlinear equations were used to check the validity of the equilibrium data of isothermal models. Equation (8) was also used to calculate the root mean square errors of each adsorbent shown in Table 3. Smaller RMSE values indicated the fitness of experimental data to the calculated one for the adsorption of BGD on unmodified and modified adsorbents.

$$\text{RMSE} = \sqrt{\sum \frac{\left(q_{e(\text{cal})} - q_{e(\text{exp})}\right)^2}{N}}. \tag{11}$$

3.6.2. Kinetics Studies. The kinetics models for the adsorption of BGD on unmodified (R-TNP and R-CLP) and chemically modified with citric acid (CA-TNP and CA-CLP) adsorbents were studied using pseudo-first-order and pseudo-second-order kinetics, shown in Figures 15 and 16, respectively.

(i) Pseudo-first-order model:

The linear form of pseudo-first-order kinetics is shown in equation (12) [88, 100] and is graphically expressed in Figure 15.

$$\ln\left(q_e - q_t\right) = \ln\left(k_1 q_e\right) - k_1 t, \tag{12}$$

where "k_1" is the rate constant for the pseudo-first-order model, q_e (mg·g^{-1}) is the amount of BGD taken at equilibrium, and q_t (mg·g^{-1}) is the amount of BGD in milligrams adsorbed on one gram of each adsorbent (adsorption of BGD on R-TNP, CA-TNP, R-CLP, and CA-CLP) at a given time per minute. From Figure 15, a linear plot between ln $(q_e - q_t)$ vs. t for the adsorption of BGD on unmodified (R-TNP and R-CLP) and citric acid-modified novel adsorbents (CA-TNP and CA-CLP) was obtained, and the pseudo-first-order parameters are displayed in Table 4. The less values of R^2 for the adsorption of BGD on each unmodified and citric acid-modified novel adsorbent indicate that the Lagergren equation (12) for the pseudo-first-order mechanism did not fit completely in a good way for the whole adsorption phenomenon.

(ii) Pseudo-second-order model:

For the pseudo-second-order mechanism, the linear form is given in equation (13) [69, 90] and is graphically expressed in Figure 16.

$$\frac{t}{q_t} = \left(\frac{1}{K_2 q_e^2}\right) + \left(\frac{t}{q_e}\right). \tag{13}$$

In equation (13), the (K_2) is the rate constant for the pseudo-second-order model which is calculated using intercept. The slope obtained from the plot (t/q_t) vs. (t) in Figure 16, gives the value of q_e.

The correlation coefficients (R^2) for the adsorption of BGD on unmodified (R-TNP and R-CLP) adsorbents are less than those on citric acid-modified novel adsorbents

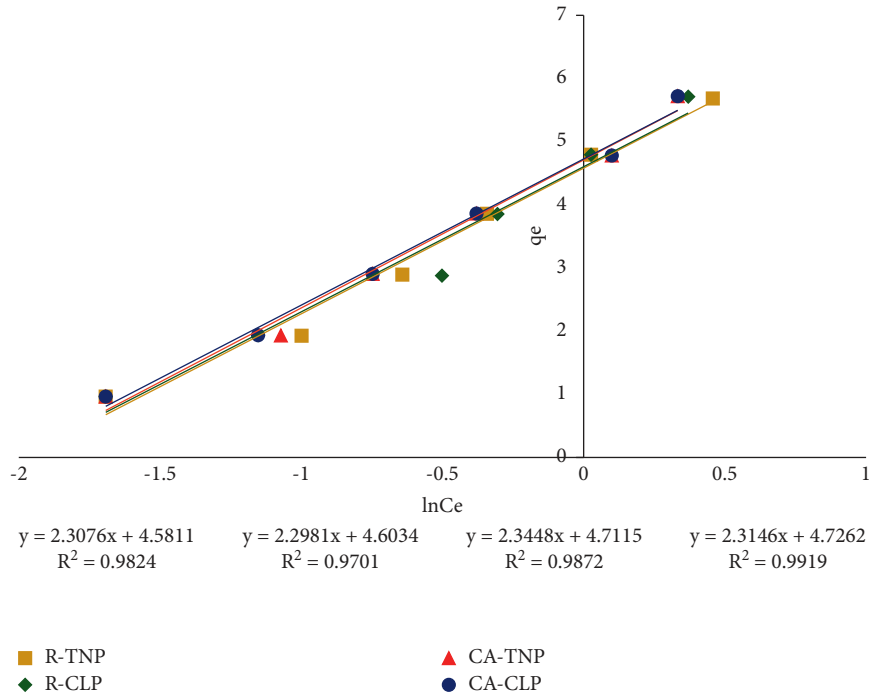

Figure 14: Comparison of effective parameters of Temkin isotherm for the adsorption of BGD. Adsorbent dose = 0.5 g, contact time- = 25 min, temperature = 30°C, agitation speed = 100 rpm, initial pH = 5, final pH: R-TNP = 5, R-CLP = 4.5, CA-TNP = 4.0, and CA-CLP = 4.0, and dye solution volume V = 100 mL.

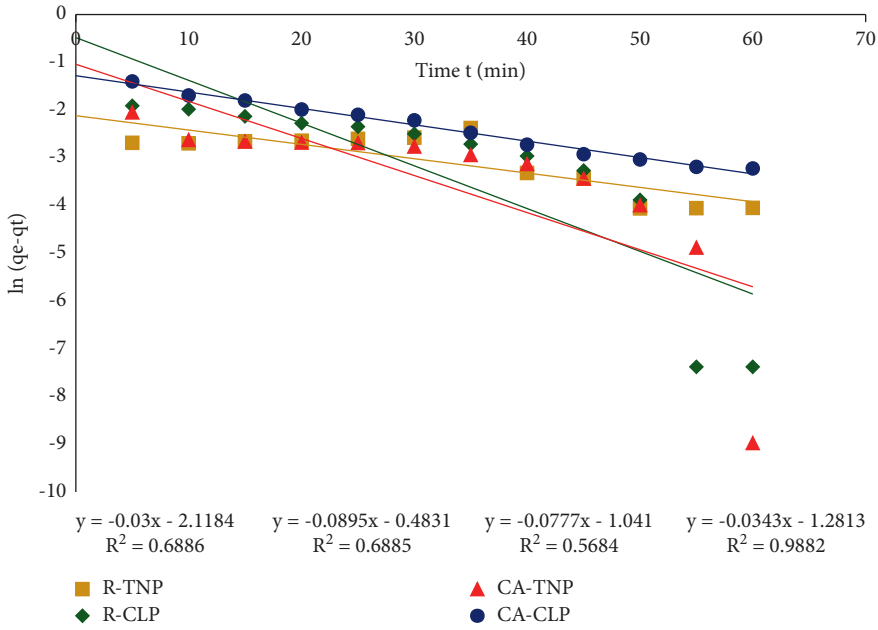

Figure 15: Comparison of pseudo-first-order kinetics for the adsorption of BGD. Time period = 5 to 60 min, adsorbent dose = 0.5 g, temperature = 30°C, agitation speed = 100 rpm, initial pH = 5, final pH: R-TNP = 5, R-CLP = 4.5, CA-TNP = 4.0, and CA-CLP = 4.0, and initial volume of the solution V = 100 mL.

(CA-TNP and CA-CLP), elaborated in Table 4. R^2 values of all adsorbents reflect the high fitness of this kinetic model than the pseudo-first-order model.

3.6.3. Root Mean Square Error and Percent Relative Deviation of Kinetic Models. Root mean square errors for kinetic models were calculated using equation (14) [101, 102]. A

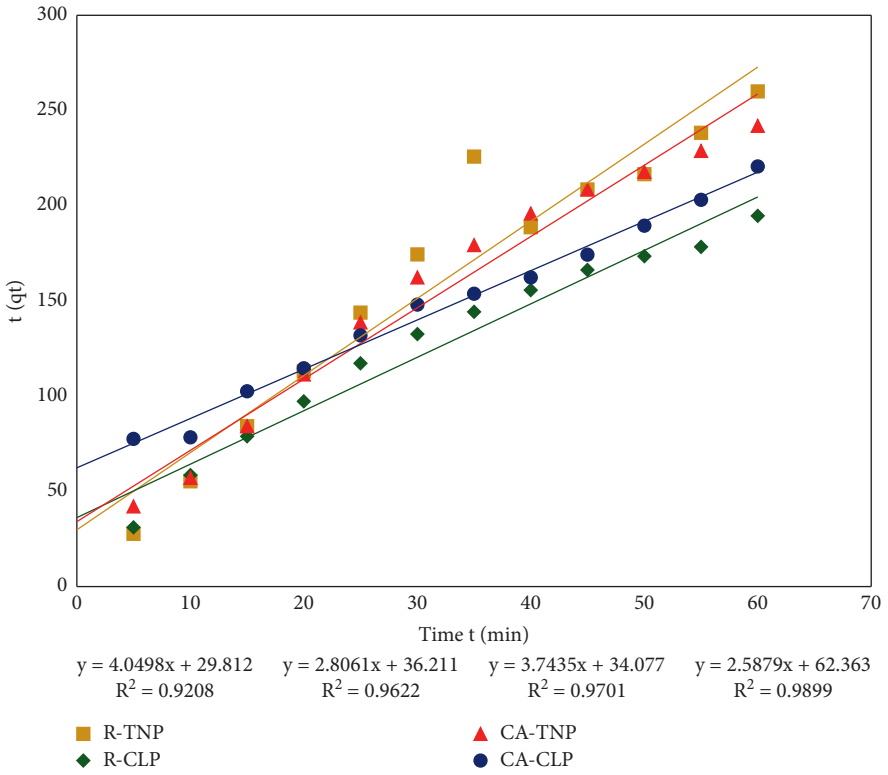

FIGURE 16: Comparison of pseudo-second-order-kinetics for adsorption. Time period = 5 to 60 min, adsorbent dose = 0.5 g, temperature = 30°C, agitation speed = 100 rpm, initial pH = 5, final pH: R-TNP = 5, R-CLP = 4.5, CA-TNP = 4.0, and CA-CLP = 4.0, and dye solution volume V = 100 mL.

comparison of the experimental RMSE results with the calculated ones indicates the more fitting of kinetic models for the adsorption of BGD on all adsorbents. These RMSE results calculated from equation (14) and shown in Table 4 have lesser values for second-order kinetics than the first order. This favors the high suitability of second-order kinetics for the adsorption of BGD on unmodified (R-TNP and R-CLP) and novel citric acid-modified (CA-TNP and CA-CLP) adsorbents.

$$\text{RMSE} = \sqrt{\sum \frac{\left(q_{t\,(\text{cal})} - q_{t\,(\text{exp})}\right)^2}{N}}, \tag{14}$$

where N is the number of observations performed and $q_{t(\text{cal})}$ and $q_{t(\text{exp})}$ are the adsorption binding capacities (mg/g) at any instant of time (t).

The percent relative deviation (P) quantitatively analyses the fitness of kinetic model during adsorption process. Lower values of percent relative deviation indicate the better fitness of the kinetic model for the adsorption studies. Percent relative deviation values for the adsorption of BGD on unmodified (R-TNP and R-CLP) and novel citric acid-modified (CA-TNP and CA-CLP) adsorbents are summarized in Table 4. For second-order kinetics, the lowest values of "P" favor its fitness and suitability for the adsorption of BGD on all adsorbents than first-order kinetics. Percent relative deviation was calculated from the following equation [103]:

$$P = \frac{100}{N} \sum \left[\frac{q_{e\,(\text{exp})} - q_{e\,(\text{cal})}}{q_{e\,(\text{exp})}}\right], \tag{15}$$

where N is the number of total observations performed, $q_{e(\text{exp})}$ is the experimental value of adsorption binding capacity, and $q_{e\,(\text{cal})}$ is the calculated value of adsorption binding capacity in (mg/g) [104].

3.6.4. Thermodynamic Approach. Figure 17 represents the comparison of thermodynamic parameters for the adsorption of BGD on unmodified adsorbents (R-TNP and R-CLP) and citric acid-modified novel adsorbents (CA-TNP and CA-CLP). The increase in temperature, directly related with the kinetic energy of brilliant green dye molecules, consequently, increases the diffusion of adsorbate (BGD) ions. This influenced and enhanced the adsorption mechanism probability due to the porous surface of lignocellulosic materials [105] (dry biomass) of R-TNP, R-CLP, CA-TNP, and CA-CLP. The Gibbs free energy (G^0), enthalpy change (H^0), and entropy of the system (S^0) are the effective thermodynamic parameters to determine the adsorption rate of BGD on unmodified and novel citric acid-modified adsorbents indicated in Table 5. The increase in negative values of Gibbs free energy with a rise in temperature determines the possibility of the adsorption process being spontaneous and exothermic at a fast rate. The higher G^0

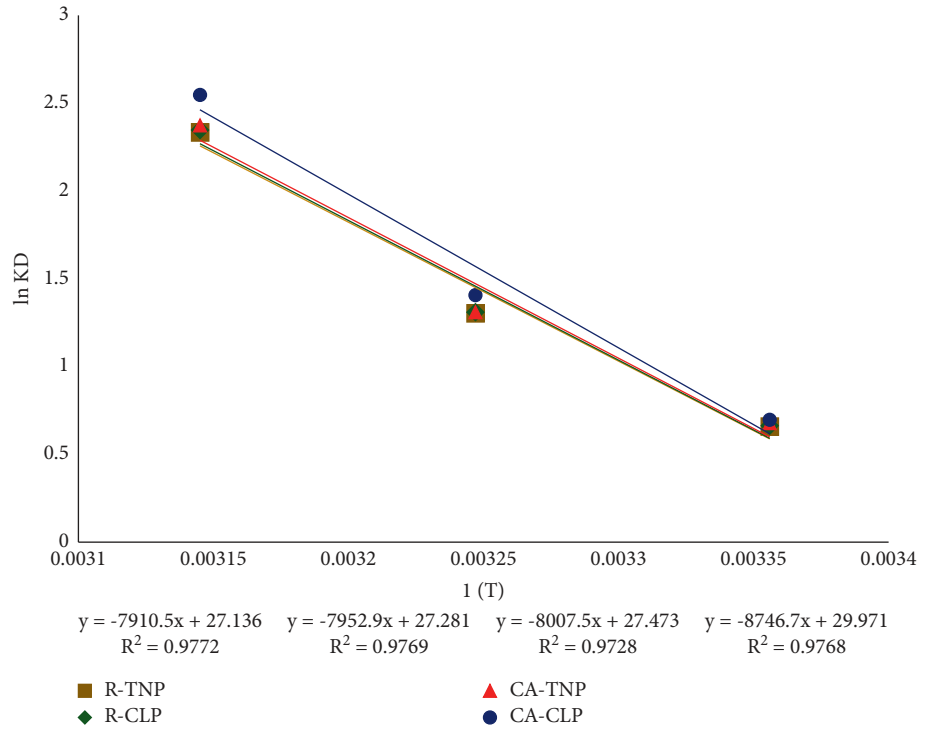

Figure 17: Comparison of thermodynamic parameters of BGD adsorption.

Table 4: A comparative study of kinetic parameters for the detoxification of BGD.

Kinetic adsorption model	R-TNP	CA-TNP (acid treated)	R-CLP	CA-CLP (acid treated)
Pseudo 1st order				
R^2	0.688	0.568	0.688	0.988
q_e (mg·g^{-1}) (exp.)	0.248	0.248	0.308	0.312
q_e (mg·g^{-1}) (cal.)	0.1202	0.3531	0.6168	0.2776
k_1 (per min.)	−0.0005	−0.0013	−0.0014	−0.00057
RMSE	5.295	7.076	6.67	13.126
P	3.97	3.288	7.717	0.838
Pseudo 2nd order				
R^2	0.92	0.97	0.96	0.99
K_2 (g·mg^{-1}·min^{-1})	0.549	0.411	0.217	0.107
q_e (mg·g^{-1}) (exp.)	0.248	0.248	0.308	0.312
q_e (mg·g^{-1}) (cal.)	0.247	0.267	0.356	0.386
RMSE	4.005	5.291	4.256	8.959
P	0.031	−0.589	−1.199	−1.855

values for novel citric acid-modified adsorbents (CA-TNP and CA-CLP) than unmodified adsorbents indicate good adsorption of BGD. This can be calculated from the following equation [106]:

$$\Delta G^0 = RT \ln K_D, \tag{16}$$

where R is the general gas constant (8.314 J·mol^{-1}K^{-1}), T is the temperature in Kelvin, and K_D is the distribution coefficient which can be calculated from the following equation:

$$K_D = \frac{C_0 - C_e}{C_e}. \tag{17}$$

The change in enthalpy determines whether the adsorption phenomenon is physical or chemical in behavior. H^0 ranging from 2.1 to 20.9 kJ·mol^{-1} determines the physical behavior of the adsorption process [107], whereas values ranging from 80 to 200 kJ·mol^{-1} indicate the chemical nature [107]. This indicates that the adsorption of BGD on all adsorbents (unmodified and novel citric acid-modified adsorbent) is chemical in nature, elaborated in Table 5. The more values of H^0 calculated from equation (18) favor this behavior for novel citric acid-modified adsorbents than their unmodified forms. Another important parameter, change in entropy (S^0), calculated from equation (18) determines the

Table 5: Thermodynamic parameters for BGD adsorption.

Biosorbents	T (K)	K_D	G^0 (Kjmol^{-1})	H^0 (Kjmol^{-1})	S^0 (Jmol^{-1}K^{-1})	Ea (KJmol^{-1})
R-TNP (untreated)	298	1.932	−1.631619251	−65.7679	225.6087	65.767
	308	3.68	−3.336384319			
	318	10.31	−6.168408903			
CA-TNP (citric acid treated)	298	1.969	−1.678618951	−66.5744	228.4105	66.574
	308	3.703	−3.352338963			
	318	10.728	−6.273483111			
R-CLP (untreated)	298	1.941	−1.643133937	−66.1204	226.8142	66.120
	308	3.703	−3.352338963			
	318	10.446	−6.203056139			
CA-CLP (citric acid treated)	298	2.006	−1.724743636	−72.7201	249.1789	72.720
	308	4.08	−3.600609431			
	318	12.768	−6.733737808			

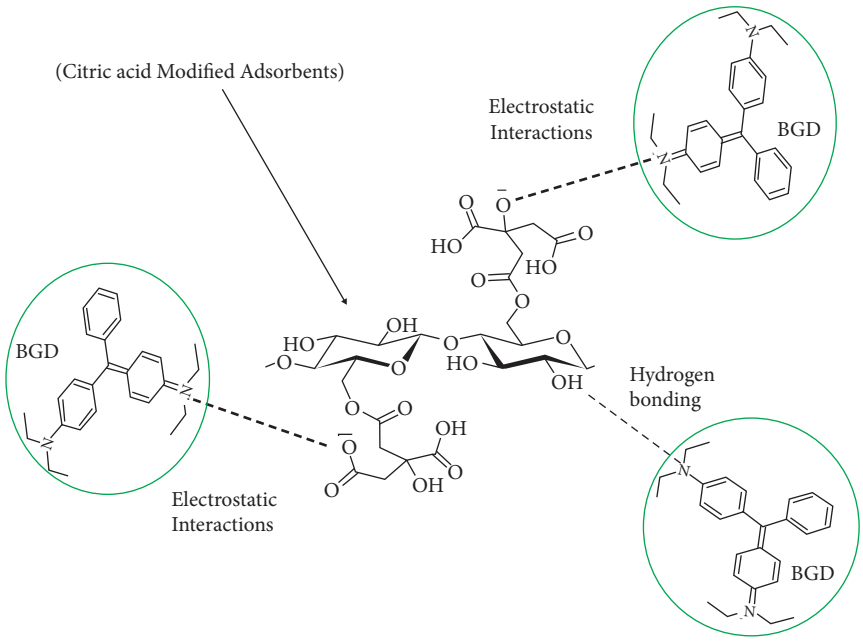

Figure 18: Schematic proposed adsorption mechanism of BGD on CA-TNP/CA-CLP.

distortedness at the solid-liquid interface in this system, and its increased positive values indicate the feasibility of the adsorption phenomenon. The linear and mathematical form of Van't Hoff equation [106, 108] is given as follows:

$$\ln K_D = \frac{\Delta S^0}{R} - \frac{\Delta H^0}{RT}. \quad (18)$$

From equation (18), it can be seen that a plot between "lnK_D" and "1/T" gives a straight line, elaborated in Figure 17.

The slope and intercept of this line were used to calculate the values of H^0 and S^0 [109] for the adsorption of BGD on unmodified (R-TNP and R-CLP) and novel citric acid-processed adsorbents (CA-TNP and CA-CLP). The higher values of S^0 indicate better adsorption of BGD on novel citric acid-modified adsorbents than their unmodified forms, summarized in Table 5. Equation (19) is used to calculate the H^0 and S^0 [110, 111]:

$$\Delta G^0 = \Delta H^0 - T\Delta S^0. \quad (19)$$

The energy of activation was calculated from the Arrhenius equation (20) for the adsorption of BGD on R-TNP, R-CLP, CA-TNP, and CA-CLP. It is important to determine whether the process of adsorption is physically or chemically controlled. Its value ranging from5 to 40 kJ·mol^{-1} indicates the physical adsorption and from 40 to 800 kJ·mol^{-1} indicates chemical adsorption [112]. In Table 5, values of E_a for the adsorption of BGD on unmodified and citric acid-modified adsorbents are summarized which indicate the physiosorption process.

$$\ln K = \ln A - \frac{E_a}{RT}, \quad (20)$$

where "K" is the rate constant, "A" is Arrhenius constant or frequency factor, R is universal gas constant (8.314 J·mol^{-1}K^{-1}), T (K), and E_a is the energy of activation (kJ·mol^{-1}) for the adsorption of BGD and was obtained from the slope of plot between ln K and 1/T.

3.7. Chemistry of Dye Removal by Chemically Treated Biomass. FTIR and SEM analysis indicated that native adsorbents' (TNP and CLP) surfaces are composed of carboxyl and hydroxyl groups. These are esterified with the citric acid during the chemical modification, and they provide additional adsorption sites to adsorb the BGD cations. A schematic proposed mechanism is shown in Figure 18. Citric acid, being a tricarboxylic acid, enhanced the acidity of the adsorbents by providing excessive carboxyl and hydroxyl groups, resulting in the decrease and maintenance of the final pH of the solution. CA-TNP detoxifies 92.6% of BGD before adsorption at pH = 5 and after adsorption at pH = 4, while CA-CLP showed high efficiency of removal of 98% BGD before adsorption at pH = 5 and after adsorption at pH = 4.5, as discussed in Section 3.5.5. Citric acid also breaks and decreases the cellulose crystallinity of lignocellulosic biomass, resulting in an increase in the porosity and surface area of TNP and CLP [66]. Total emplacement sites on the biosorbent surface can be increased by providing additional functional groups during the chemical treatment with suitable modifying agents [67, 68]. Thus, the surface of adsorbents favor more electrostatic and hydrogen bonding interactions with the cationic molecules of BGD due to the presence of a lot of negatively active binding sites on them. Hence, the citric acid chemical-processed *Trapa natans* and *Citrullus lanatus* peels as novel adsorbents showed more favorable, efficient, and good results during this investigation. A comparison of the adsorption efficiency of novel citric acid-modified biosorbents with that of the previously reported biosorbents is shown in Table 1.

3.8. Desorption and Regeneration of Biosorbents. For the regeneration of adsorbents, desorption studies of used samples were carried out. Various eluents were used to investigate better and efficient results for the desorption of BGD and regeneration of TNP and CLP for their further use in adsorption. For this purpose, various concentrations of 0.01, 0.05, and 0.1 molar acidic solutions of each HCl, H_2SO_4, and HNO_3, respectively, were used to provide acidic media, while various concentrations of 0.01, 0.05, and 0.1 molar basic solutions of NaOH and KOH were employed to provide basic media. It was investigated during this study that 0.1 M NaOH eluent gave the maximum desorption efficiency of 88% for BGD-R-TNP, 86.7% for BGD-R-CLP, 84% for BGD-CA-TNP, and 89.6% for BGD-CA-CLP. It was also observed that as the number of recycling experiments increases, the adsorption capacity of regenerated adsorbents decreases.

4. Conclusions

It was investigated experimentally that low cost, easily, and abundantly available ecofriendly chemically processed, citric acid-modified *Trapa natans* peels and *Citrullus lanatus* peels showed efficient adsorption capabilities against cationic, hazardous, and toxic model brilliant green dye, as compared to their unmodified and native forms. These were characterized by FTIR and SEM for their surface morphology to identify the various functional groups such as -OH and -COOH and NH_2 groups. It was observed that citric acid-modified novel adsorbents have more acidic groups for better adsorption than their unmodified forms. From the comparative study of mathematical isothermal models, Langmuir, Freundlich, and Temkin, it was found, that the adsorption phenomenon was more efficiently followed by Langmuir isotherm due to high values of q_{max} for novel citric acid chemically modified adsorbents, providing more negatively binding sites than their unmodified forms (q_{max} for CA-TNP 128 $mg{\cdot}g^{-1}$ than its unmodified form R-TNP 108.6 $mg{\cdot}g^{-1}$ while CA-CLP 188.68 $mg{\cdot}g^{-1}$ than its native form R-CLP 144.9 $mg{\cdot}g^{-1}$). High regression coefficients and R^2 of Langmuir isotherm for citric acid-modified adsorbents indicate that the adsorption phenomenon is monolayer, homogeneous, and associated with chemisorption due to esterification reaction. Temkin isotherm indicates the physical behavior of adsorption process. The pseudo-second-order kinetic model fits well than the pseudo-first-order kinetic model, and negative ΔG^0 values of all adsorbents determine that the adsorption phenomenon is exothermic and spontaneous in nature. The other thermodynamic parameters, enthalpy change (H^0), entropy of the system (S^0), and energy of activation (E_a), indicated the more efficient physicochemical adsorption of BGD on novel citric acid-modified adsorbent, CA-TNP and CA-CLP, than their unmodified forms, R-TNP and R-CLP. From the adsorption efficiency and compared with the previously reported biosorbents, it is concluded that novel citric acid chemically modified *Trapa natans* peels and *Citrullus lanatus* peels have better capability to eradicate brilliant green dye from aqueous media than their native and raw forms.

Abbreviations

FTIR: Fourier transform infrared spectroscopy
SEM: Scanning electron microscopy
pZC pH: Point of zero charge
BGD: Brilliant green dye
TNP: *Trapa natans* peels
CLP: *Citrullus lanatus* peels
CA-TNP: Citric acid-modified *Trapa natans* peels (novel adsorbent)
CA-CLP: Citric acid-modified *Citrullus lanatus* peels (novel adsorbent).

Data Availability

All data related to this work are presented in the article.

Conflicts of Interest

The authors have no conflicts of interest regarding the publication of this paper.

Acknowledgments

The authors are thankful to COMSAT, Lahore, and LUMS for analysis services. They are thankful to Home Institute for funding this work.

References

[1] W. Larry, *A Billion People Worldwide Lack Safe Drinking Water*, 2006, http://www.environment.about.com/od/ environmentalevents/.

[2] R. Rehman and W. Luqman, "Removal of basic blue-9 dye from water by Eugenia jambolana seeds and Citrullus lanatus peels," *Asian Journal of Chemistry*, vol. 26, no. 13, pp. 3827–3832, 2014.

[3] R. Rehman, T. Mahmud, and J. Anwar, "Isothermal modeling of batch biosorption of brilliant green dye from water by chemically modified Eugenia," *Journal of the Chemical Society of Pakistan*, vol. 34, no. 1, p. 136, 2012.

[4] S. Latif, R. Rehman, M. Imran, M. S. Hussain, S. Iqbal, and L. Mitu, "Removal of cadmium (II) and lead (II) from water by chemically treated Citrullus lanatus peels as biosorbent in cost effective way," *Revista de Chimie*, vol. 71, pp. 182–192, 2020.

[5] N. Ali, Ikramullah, G. Lutfullah, A. Hameed, and S. Ahmed, "Decolorization of acid red 151 by Aspergillus niger SA1 under different physicochemical conditions," *World Journal of Microbiology and Biotechnology*, vol. 24, no. 7, pp. 1099–1105, 2008.

[6] J. Huang, D. Liu, J. Lu, H. Wang, X. Wei, and J. Liu, "Biosorption of reactive black 5 by modified Aspergillus versicolor biomass: kinetics, capacity and mechanism studies," *Colloids and Surfaces A: Physicochemical and Engineering Aspects*, vol. 492, pp. 242–248, 2016.

[7] H. Wang, X. Yuan, Z. Wu et al., "Removal of basic dye from aqueous solution using Cinnamomum camphora sawdust: kinetics, isotherms, thermodynamics, and mass-transfer processes," *Separation Science and Technology*, vol. 49, no. 17, pp. 2689–2699, 2014.

[8] T. A. Khan, S. Dahiya, and I. Ali, "Removal of direct red 81 dye from aqueous solution by native and citric acid modified bamboo sawdust—kinetic study and equilibrium isotherm analyses," *Gazi University Journal of Science*, vol. 25, no. 1, 2012.

[9] J.-Z. Guo, B. Li, L. Liu, and K. Lv, "Removal of methylene blue from aqueous solutions by chemically modified bamboo," *Chemosphere*, vol. 111, pp. 225–231, 2014.

[10] Y. Fu and T. Viraraghavan, "Fungal decolorization of dye wastewaters: a review," *Bioresource Technology*, vol. 79, no. 3, pp. 251–262, 2001.

[11] A. Demirbas, "Agricultural based activated carbons for the removal of dyes from aqueous solutions: a review," *Journal of Hazardous Materials*, vol. 167, no. 1–3, pp. 1–9, 2009.

[12] M. T. Yagub, T. K. Sen, and H. M. Ang, "Equilibrium, kinetics, and thermodynamics of methylene blue adsorption by pine tree leaves," *Water, Air, & Soil Pollution*, vol. 223, no. 8, pp. 5267–5282, 2012.

[13] R. Jayashree, "Biodegradation capability of bacterial species isolated from oil contaminated soil," *Journal of Academia and Industrial Research*, vol. 1, no. 3, pp. 127–135, 2012.

[14] Z. Al-Qodah, "Adsorption of dyes using shale oil ash," *Water Research*, vol. 34, no. 17, pp. 4295–4303, 2000.

[15] H. Ashfaq, "*Green synthesis of silver nanocomposites from powders of various medicinal plants and study of their antimicrobial potential*," M.S. thesis, COMSATS University Islamabad, Islamabad, Pakistan, 2021.

[16] R. Rehman, B. Salariya, and L. Mitu, "Batch scale adsorptive removal of brilliant green dye using Trapa natans peels in cost effective manner," *Revue Chimique*, vol. 67, pp. 1333–1337, 2016.

[17] C. Deshmukh, A. Jain, and M. S. Tambe, "Phytochemical and pharmacological profile of Citrullus lanatus (THUNB)," *Biolife*, vol. 3, no. 2, pp. 483–488, 2015.

[18] W. Gin, "Production of activated carbon from watermelon peel," *International Journal of Scientific and Engineering Research*, vol. 5, pp. 66–71, 2014.

[19] J. K. Patra, G. Das, and K.-H. Baek, "Phyto-mediated biosynthesis of silver nanoparticles using the rind extract of watermelon (Citrullus lanatus) under photo-catalyzed condition and investigation of its antibacterial, anticandidal and antioxidant efficacy," *Journal of Photochemistry and Photobiology B: Biology*, vol. 161, pp. 200–210, 2016.

[20] Y. Kismir and A. Z. Aroguz, "Adsorption characteristics of the hazardous dye brilliant green on Saklikent mud," *Chemical Engineering Journal*, vol. 172, no. 1, pp. 199–206, 2011.

[21] A. Ragab, I. Ahmed, and D. Bader, "The removal of brilliant green dye from aqueous solution using nano hydroxyapatite/chitosan composite as a sorbent," *Molecules*, vol. 24, no. 5, p. 847, 2019.

[22] M. S. U. Rehman, M. Munir, M. Ashfaq et al., "Adsorption of brilliant green dye from aqueous solution onto red clay," *Chemical Engineering Journal*, vol. 228, pp. 54–62, 2013.

[23] R. Rehman, S. J. Muhammad, and M. Arshad, "Brilliant green and acid orange 74 dyes removal from water by Pinus roxburghii leaves in naturally benign way: an application of green chemistry," *Journal of Chemistry*, vol. 2019, Article ID 3573704, 10 pages, 2019.

[24] U. S. Orlando, A. U. Baes, W. Nishijima, and M. Okada, "Preparation of chelating agents from sugarcane bagasse by microwave radiation as an alternative ecologically benign procedure," *Green Chemistry*, vol. 4, no. 6, pp. 555–557, 2002.

[25] R. Rehman, J. Anwar, and T. Mahmud, "Thermodynamical and isothermal modeling of methylene blue dye batch biosorption on formalin modified madhuca," *Journal of the Chemical Society of Pakistan*, vol. 34, no. 2, p. 460, 2012.

[26] O. Ekpete and M. Horsfall, "Preparation and characterization of activated carbon derived from fluted pumpkin stem waste (Telfairia occidentalis Hook F)," *Research Journal of Chemical Sciences*, vol. 1, no. 3, pp. 10–17, 2011.

[27] Y. Chen, Y. Zhu, Z. Wang et al., "Application studies of activated carbon derived from rice husks produced by chemical-thermal process—a review," *Advances in Colloid and Interface Science*, vol. 163, no. 1, pp. 39–52, 2011.

[28] A. Hashem, S. M. Badawy, S. Farag, L. A. Mohamed, A. J. Fletcher, and G. M. Taha, "Non-linear adsorption characteristics of modified pine wood sawdust optimised for adsorption of Cd(II) from aqueous systems," *Journal of Environmental Chemical Engineering*, vol. 8, no. 4, Article ID 103966, 2020.

[29] Z. Abootorabi, M. R. Sohrabi, and S. Mortazavinik, "Removing diazo direct red 81 using chitosan/zero-valent iron nanocomposite from aqueous solutions and process optimization," *International Journal of Environmental Analytical Chemistry*, pp. 1–18, 2021.

[30] B. Asmaa, A. Morsli, E. Guibal, and R. Kessas, "New derivatives of urea-grafted alginate for improving the sorption of mercury ions in aqueous solutions," *Materials Research Express*, vol. 8, Article ID 035303, 2021.

[31] M. Salman, R. Rehman, U. Farooq, A. Tahir, and L. Mitu, "Biosorptive removal of cadmium(II) and copper(II) using microwave-assisted thiourea-modified sorghum bicolor

agrowaste," *Journal of Chemistry*, vol. 2020, Article ID 8269643, 11 pages, 2020.

[32] K. Zhang, Z. Dai, W. Zhang et al., "EDTA-based adsorbents for the removal of metal ions in wastewater," *Coordination Chemistry Reviews*, vol. 434, Article ID 213809, 2021.

[33] Y. Feng, H. Zhou, G. Liu et al., "Methylene blue adsorption onto swede rape straw (Brassica napus L.) modified by tartaric acid: equilibrium, kinetic and adsorption mechanisms," *Bioresource Technology*, vol. 125, pp. 138–144, 2012.

[34] S. M. Ghasemi, "Adsorption of basic blue3 (BB3) dye from aqueous solution by tartaric acid modified sunflower stem: kinetics and equilibrium studies," *International Research Journal of Applied and Basic Sciences*, vol. 9, no. 5, pp. 686–694, 2015.

[35] M. O. Saleh, M. A. Hashem, and M. Akl, "Removal of Hg (II) metal ions from environmental water samples using chemically modified natural sawdust," *Egyptian Journal of Chemistry*, vol. 64, no. 2, pp. 1027–1034, 2021.

[36] L. Chen, A. Ramadan, L. Lü, W. Shao, F. Luo, and J. Chen, "Biosorption of methylene blue from aqueous solution using lawny grass modified with citric acid," *Journal of Chemical & Engineering Data*, vol. 56, no. 8, pp. 3392–3399, 2011.

[37] A. Essekri, N. Aarab, A. Hsini et al., "Enhanced adsorptive removal of crystal violet dye from aqueous media using citric acid modified red-seaweed: experimental study combined with RSM process optimization," *Journal of Dispersion Science and Technology*, pp. 1–14, 2020.

[38] I. M. Kenawy, W. I. Mortada, Y. G. A. El-Reash, and A. A. Mousa, "Preparation of lactic acid modified cellulose nanoparticles by microwave heating for preconcentration of copper from blood and food samples," *Environmental Science and Pollution Research*, vol. 27, no. 7, pp. 7256–7266, 2020.

[39] H. Li, Z. Yuan, Y. Xing et al., "Acetone fractionation: a simple and efficient method to improve the performance of lignin for dye pollutant removal," *RSC Advances*, vol. 9, no. 61, pp. 35895–35903, 2019.

[40] N. Almoisheer, F. A. Alseroury, R. Kumar, T. Almeelbi, and M. A. Barakat, "Synthesis of graphene oxide/silica/carbon nanotubes composite for removal of dyes from wastewater," *Earth Systems and Environment*, vol. 3, no. 3, pp. 651–659, 2019.

[41] N. M. Nor, "Removal of brilliant green and procionred dyes from aqueous solution by adsorption using selected agricultural wastes," *Jurnal Teknologi*, vol. 74, no. 11, 2015.

[42] R. Ahmad and P. K. Mondal, "Application of acid treated almond peel for removal and recovery of brilliant green from industrial wastewater by column operation," *Separation Science and Technology*, vol. 44, no. 7, pp. 1638–1655, 2009.

[43] M. K. Dahri, L. B. Lim, and C. C. Mei, "Cempedak durian as a potential biosorbent for the removal of brilliant green dye from aqueous solution: equilibrium, thermodynamics and kinetics studies," *Environmental Monitoring and Assessment*, vol. 187, no. 8, pp. 546–613, 2015.

[44] R. Fiaz, M. Hafeez, and R. Mahmood, "Removal of brilliant green (BG) from aqueous solution by using low cost biomass Salix alba leaves (SAL): thermodynamic and kinetic studies," *Journal of Water Reuse and Desalination*, vol. 10, no. 1, pp. 70–81, 2020.

[45] L. T. Popoola, A. S. Yusuff, O. A. Adesina, and M. A. Lala, "Brilliant green dye sorption onto snail shell-rice husk: statistical and error function models as parametric isotherm predictors," *Journal of Environmental Science and Technology*, vol. 12, no. 2, pp. 65–80, 2019.

[46] M. Ashrafi, "Removal of brilliant green and crystal violet from mono-and bi-component aqueous solutions using NaOH-modified walnut shell," *Analytical and Bioanalytical Chemistry Research*, vol. 5, no. 1, pp. 95–114, 2018.

[47] N. A. H. M. Zaidi, L. W. Jing, and L. B. Lim, "Adsorption of brilliant green dye on Nephelium mutabile (Pulasan) leaves," *Scientia Bruneiana*, vol. 17, no. 1, 2018.

[48] S. Agarwal, V. K. Gupta, M. Ghasemi, and J. Azimi-Amin, "Peganum harmala -L seeds adsorbent for the rapid removal of noxious brilliant green dyes from aqueous phase," *Journal of Molecular Liquids*, vol. 231, pp. 296–305, 2017.

[49] N. Laskar and U. Kumar, "Removal of brilliant green dye from water by modified Bambusa tulda: adsorption isotherm, kinetics and thermodynamics study," *International journal of Environmental Science and Technology*, vol. 16, no. 3, pp. 1649–1662, 2019.

[50] O. S. Esan, O. N. Abiola, O. Owoyomi, C. O. Aboluwoye, and M. O. Osundiya, "Adsorption of brilliant green onto Luffa cylindrical sponge: equilibrium, kinetics, and thermodynamic studies," *International Scholarly Research Notices*, vol. 2014, Article ID 743532, 12 pages, 2014.

[51] M. El Hajam, N. I. Kandri, and A. Zerouale, "Batch adsorption of brilliant green dye on raw Beech sawdust: equilibrium isotherms and kinetic studies," *Moroccan Journal of Chemistry*, vol. 7, no. 3, pp. 431–435, 2019.

[52] R. Kumar and M. A. Barakat, "Decolourization of hazardous brilliant green from aqueous solution using binary oxidized cactus fruit peel," *Chemical Engineering Journal*, vol. 226, pp. 377–383, 2013.

[53] M. Ghaedi, H. Hossainian, M. Montazerozohori et al., "A novel acorn based adsorbent for the removal of brilliant green," *Desalination*, vol. 281, pp. 226–233, 2011.

[54] R. Ahmad and K. Ansari, "Chemically treated Lawsonia inermis seeds powder (CTLISP): an eco-friendly adsorbent for the removal of brilliant green dye from aqueous solution," *Groundwater for Sustainable Development*, vol. 11, Article ID 100417, 2020.

[55] T. Calvete, "Removal of brilliant green dye from aqueous solutions using home made activated carbons," *Clean—Soil, Air, Water*, vol. 38, no. 5-6, pp. 521–532, 2010.

[56] R. Lakshmipathy, N. A. Reddy, and N. C. Sarada, "Optimization of brilliant green biosorption by native and acid-activated watermelon rind as low-cost adsorbent," *Desalination and Water Treatment*, vol. 54, no. 1, pp. 235–244, 2015.

[57] C. Karthik, V. S. Ramkumar, A. Pugazhendhi, K. Gopalakrishnan, and P. I. Arulselvi, "Biosorption and biotransformation of Cr(VI) by novel Cellulosimicrobium funkei strain AR6," *Journal of the Taiwan Institute of Chemical Engineers*, vol. 70, pp. 282–290, 2017.

[58] A. Hashem, E. S. Abdel-Halim, K. F. El-Tahlawy, and A. Hebeish, "Enhancement of the adsorption of Co(II) and Ni(II) ions onto peanut hulls through esterification using citric acid," *Adsorption Science and Technology*, vol. 23, no. 5, pp. 367–380, 2005.

[59] O. S. Bello, O. C. Alao, T. C. Alagbada, O. S. Agboola, O. T. Omotoba, and O. R. Abikoye, "A renewable, sustainable and low-cost adsorbent for ibuprofen removal," *Water Science and Technology*, vol. 83, no. 1, pp. 111–122, 2021.

[60] X. He, F. Luzi, W. Yang et al., "Citric acid as green modifier for tuned hydrophilicity of surface modified cellulose and lignin nanoparticles," *ACS Sustainable Chemistry & Engineering*, vol. 6, no. 8, pp. 9966–9978, 2018.

[61] N. D. Thanh and H. L. Nhung, "Cellulose modified with citric acid and its absorption of Pb2+ and Cd2+ ions," in *Proceedings of the 13th International Electronic Conference on Synthetic Organic Chemistr*, Riga, Latvia, 2009.

[62] M. Tamez Uddin, M. Rukanuzzaman, M. Maksudur Rahman Khan, and M. Akhtarul Islam, "Adsorption of methylene blue from aqueous solution by jackfruit (Artocarpus heteropyllus) leaf powder: a fixed-bed column study," *Journal of Environmental Management*, vol. 90, no. 11, pp. 3443–3450, 2009.

[63] H. N. Tran, S.-J. You, T. V. Nguyen, and H.-P. Chao, "Insight into the adsorption mechanism of cationic dye onto biosorbents derived from agricultural wastes," *Chemical Engineering Communications*, vol. 204, no. 9, pp. 1020–1036, 2017.

[64] M. Singh, D. Tiwari, and M. Bhagat, "Batch adsorption studies on the removal of amaranth red dye from aqueous solution using activated Trapa natans peels," *Pollution Research*, vol. 39, 2020.

[65] A. H. Jawad, Y. S. Ngoh, and K. A. Radzun, "Utilization of watermelon (Citrullus lanatus) rinds as a natural low-cost biosorbent for adsorption of methylene blue: kinetic, equilibrium and thermodynamic studies," *Journal of Taibah University for Science*, vol. 12, no. 4, pp. 371–381, 2018.

[66] C. Sun, "Characterization of citric acid-modified clam shells and application for aqueous lead (II) removal," vol. 227, no. 9, pp. 1–11, 2016.

[67] R. Aguado, A. F. Lourenço, P. J. T. Ferreira, A. Moral, and A. Tijero, "The relevance of the pretreatment on the chemical modification of cellulosic fibers," *Cellulose*, vol. 26, no. 10, pp. 5925–5936, 2019.

[68] S. Basharat, R. Rehman, and L. Mitu, "Adsorptive separation of brilliant green dye from water by tartaric acid-treated holarrhena antidysenterica and Citrullus colocynthis biowaste," *Journal of Chemistry*, vol. 2021, Article ID 6636181, 18 pages, 2021.

[69] S. Afshin, Y. Rashtbari, M. Vosoughi et al., "Removal of basic blue-41 dye from water by stabilized magnetic iron nanoparticles on clinoptilolite zeolite," *Revista de Chimie*, vol. 71, no. 2, pp. 218–229, 2020.

[70] S. Kanamarlapudi, V. K. Chintalpudi, and S. Muddada, "Application of biosorption for removal of heavy metals from wastewater," *Biosorption*, vol. 18, pp. 69–116, 2018.

[71] M. R. Kahkha, M. Kaykhaii, and G. Ebrahimzadeh, "Optimization of affective parameter on cadmium removal from an aqueous solution by Citrullus colocynthis powdered fruits by response surface," *Health Scope*, vol. 4, no. 1, 2015.

[72] K. Sukla Baidya and U. Kumar, "Adsorption of brilliant green dye from aqueous solution onto chemically modified areca nut husk," *South African Journal of Chemical Engineering*, vol. 35, pp. 33–43, 2021.

[73] M. Raluca, R. Hlihor, L. Bulgariu et al., "Recent advances in biosorption of heavy metals: support tools for biosorption equilibrium, kinetics and mechanism," *Revue Roumaine de Chimie*, vol. 59, pp. 527–538, 2014.

[74] L. Zhang, L. Sellaoui, D. Franco et al., "Adsorption of dyes brilliant blue, sunset yellow and tartrazine from aqueous solution on chitosan: analytical interpretation via multilayer statistical physics model," *Chemical Engineering Journal*, vol. 382, Article ID 122952, 2020.

[75] D. Park, Y.-S. Yun, and J. M. Park, "The past, present, and future trends of biosorption," *Biotechnology and Bioprocess Engineering*, vol. 15, no. 1, pp. 86–102, 2010.

[76] W. A. Moats, J. A. Kinner, and S. E. Maddox Jr., "Effect of heat on the antimicrobial activity of brilliant green dye," *Applied Microbiology*, vol. 27, no. 5, pp. 844–847, 1974.

[77] S. K. Ghosh and A. Bandyopadhyay, "Adsorption of methylene blue onto citric acid treated carbonized bamboo leaves powder: equilibrium, kinetics, thermodynamics analyses," *Journal of Molecular Liquids*, vol. 248, pp. 413–424, 2017.

[78] R. Dandge, "Removal of methylene blue using thick rind of water melon as an adsorbent," vol. 5, no. 3, pp. 272–282, 2016.

[79] U. A. Saed, M. H. A. Nahrain, and A. A. Atshan, "Adsorption of methylene blue dye from aqueous solution using can papyrus," *Journal of Babylon University/Engineering Sciences*, vol. 22, no. 1, pp. 218–229, 2014.

[80] M. A. Barakat, R. Kumar, M. Balkhyour, and M. A. Taleb, "Novel Al_2O_3/GO/halloysite nanotube composite for sequestration of anionic and cationic dyes," *RSC Advances*, vol. 9, no. 24, pp. 13916–13926, 2019.

[81] Y. Önal, "Adsorption kinetics of malachite green onto activated carbon prepared from Tunçbilek lignite," *Journal of Hazardous Materials*, vol. 128, no. 2-3, pp. 150–157, 2006.

[82] A. Chham, "The use of insoluble mater of Moroccan oil shale for removal of dyes from aqueous solution," *Chemistry International*, vol. 4, no. 1, pp. 67–77, 2018.

[83] A. Gouza, K. Fanidi, S. Saoiabi, A. Laghzizil, and A. Saoiabi, "Effect of heat treatment on the surface properties of selected bituminous shale for cationic dye sorption," *Desalination and Water Treatment*, vol. 66, pp. 274–280, 2017.

[84] T. A. Khan, M. Nazir, and E. A. Khan, "Adsorptive removal of rhodamine B from textile wastewater using water chestnut (Trapa natans L.) peel: adsorption dynamics and kinetic studies," *Toxicological and Environmental Chemistry*, vol. 95, no. 6, pp. 919–931, 2013.

[85] V. Joshi, J. C. Mitra, and S. K. sar, "Analysis of watermelon peel and lemon peel as low cost noval bioadsorbents," *Journal of University of Shanghai for Science and Technology*, vol. 22, no. 11, pp. 483–499, 2020.

[86] S. Pandey, J. Y. Do, J. Kim, and M. Kang, "Fast and highly efficient removal of dye from aqueous solution using natural locust bean gum based hydrogels as adsorbent," *International Journal of Biological Macromolecules*, vol. 143, pp. 60–75, 2020.

[87] R. Mansour, A. El Shahawy, A. Attia, and M. S. Beheary, "Brilliant green dye biosorption using activated carbon derived from guava tree wood," *International Journal of Chemical Engineering*, vol. 2020, Article ID 8053828, 12 pages, 2020.

[88] T. W. Weber and R. K. Chakravorti, "Pore and solid diffusion models for fixed-bed adsorbers," *AIChE Journal*, vol. 20, no. 2, pp. 228–238, 1974.

[89] R. Rehman, "Comparative removal of Congo red dye from water by adsorption on Grewia asiatica leaves, Raphanus sativus peels and," *Journal of the Chemical Society of Pakistan*, vol. 34, no. 1, p. 112, 2012.

[90] J. N. Wekoye, W. C. Wanyonyi, P. T. Wangila, and M. K. Tonui, "Kinetic and equilibrium studies of Congo red dye adsorption on cabbage waste powder," *Environmental Chemistry and Ecotoxicology*, vol. 2, pp. 24–31, 2020.

[91] Y. El Maguana, N. Elhadiri, M. Benchanaa, and R. Chikri, "Activated carbon for dyes removal: modeling and understanding the adsorption process," *Journal of Chemistry*, vol. 2020, Article ID 2096834, 9 pages, 2020.

[92] D. Balarak, F. Mostafapour, H. Azarpira, and A. Joghataei, "Langmuir, Freundlich, Temkin and Dubinin-radushkevich isotherms studies of equilibrium sorption of ampicilin unto montmorillonite nanoparticles," *Journal of Pharmaceutical Research International*, vol. 20, no. 2, pp. 1–9, 2017.

[93] A. Dada, "Langmuir, Freundlich, Temkin and Dubinin-Radushkevich isotherms studies of equilibrium sorption of Zn2+ unto phosphoric acid modified rice husk," *IOSR Journal of Applied Chemistry*, vol. 3, no. 1, pp. 38–45, 2012.

[94] V. S. Munagapati, J.-C. Wen, C.-L. Pan, Y. Gutha, J.-H. Wen, and G. M. Reddy, "Adsorptive removal of anionic dye (reactive black 5) from aqueous solution using chemically modified banana peel powder: kinetic, isotherm, thermodynamic, and reusability studies," *International Journal of Phytoremediation*, vol. 22, no. 3, pp. 267–278, 2020.

[95] Y. Ho, "Review of second-order models for adsorption systems," *Journal of Hazardous Materials*, vol. 136, no. 3, pp. 681–689, 2006.

[96] J.-J. Lee, "Characteristics of isotherm, kinetic and thermodynamic parameters for the adsorption of acid red 66 by activated carbon," *Clean Technology*, vol. 26, no. 1, pp. 30–38, 2020.

[97] Y. S. Ho and G. McKay, "Sorption of dye from aqueous solution by peat," *Chemical Engineering Journal*, vol. 70, no. 2, pp. 115–124, 1998.

[98] A. S. Muhammad, "Adsorption of methylene blue onto modified agricultural waste," *Moroccan Journal of Chemistry*, vol. 8, no. 2, pp. 412–427, 2020.

[99] C. A. Igwegbe, "Equilibrium and kinetics analysis on vat yellow 4 uptake from aqueous environment by modified rubber seed shells: nonlinear modelling," *Journal of Materials and Environmental Science*, vol. 11, no. 9, pp. 1424–1444, 2020.

[100] S. Basharat, R. Rehman, T. Mahmud, S. Basharat, and L. Mitu, "Tartaric acid-modified Holarrhena antidysenterica and Citrullus colocynthis biowaste for efficient eradication of crystal violet dye from water," *Journal of Chemistry*, vol. 2020, Article ID 8862167, 18 pages, 2020.

[101] S. Bapat, D. Jaspal, and A. Malviya, "Efficacy of parthenium hysterophorus waste biomass compared with activated charcoal for the removal of CI reactive red 239 textile dye from wastewater," *Coloration Technology*, vol. 137, pp. 234–250, 2021.

[102] C. S. Bețianu, P. Cosma, M. Roşca, E.-D. Comăniță Ungureanu, I. Mămăligă, and M. Gavrilescu, "Sorption of organic pollutants onto soils: surface diffusion mechanism of Congo red azo dye," *Processes*, vol. 8, no. 12, p. 1639, 2020.

[103] K. Riahi, S. Chaabane, and B. B. Thayer, "A kinetic modeling study of phosphate adsorption onto Phoenix dactylifera L. date palm fibers in batch mode," *Journal of Saudi Chemical Society*, vol. 21, pp. S143–S152, 2017.

[104] R. A. K. Rao and M. A. Khan, "Removal and recovery of Cu(II), Cd(II) and Pb(II) ions from single and multimetal systems by batch and column operation on neem oil cake (NOC)," *Separation and Purification Technology*, vol. 57, no. 2, pp. 394–402, 2007.

[105] Y. Li, B. Xing, Y. Ding, X. Han, and S. Wang, "A critical review of the production and advanced utilization of biochar via selective pyrolysis of lignocellulosic biomass," *Bioresource Technology*, vol. 312, Article ID 123614, 2020.

[106] S. Shakoor and A. Nasar, "Utilization of Punica granatum peel as an eco-friendly biosorbent for the removal of methylene blue dye from aqueous solution," *Journal of Applied Biotechnology & Bioengineering*, vol. 5, pp. 242–249, 2018.

[107] Y. Liu and Y.-J. Liu, "Biosorption isotherms, kinetics and thermodynamics," *Separation and Purification Technology*, vol. 61, no. 3, pp. 229–242, 2008.

[108] M. Aljohani and H. A. Al-Aoh, "Adsorptive removal of permanganate anions from synthetic wastewater using copper sulfide nanoparticles," *Materials Research Express*, vol. 8, Article ID 035012, 2021.

[109] T. Muthulakshmi, M. A. M. Thangam, and C. Kannan, "Environmental toxicity assessment on organic dyes using Typha angustata," *Journal of Environmental Nanotechnology*, vol. 7, no. 2, pp. 37–44, 2018.

[110] A. A. Basirun, "Thermodynamic alternative calculations on a published work on adsorption of methyl orange using chitosan intercalated montmorillonite," *Bioremediation Science and Technology Research*, vol. 8, no. 2, pp. 12–15, 2020.

[111] K. G. Bhattacharyya and A. Sharma, "Azadirachta indica leaf powder as an effective biosorbent for dyes: a case study with aqueous congo red solutions," *Journal of Environmental Management*, vol. 71, no. 3, pp. 217–229, 2004.

[112] I. Tan, A. Ahmad, and B. Hameed, "Enhancement of basic dye adsorption uptake from aqueous solutions using chemically modified oil palm shell activated carbon," *Colloids and Surfaces A: Physicochemical and Engineering Aspects*, vol. 318, no. 1–3, pp. 88–96, 2008.